U.S. DEPARTMENT OF COMMERCE
National Technical Information Service

PB-259 877

Stack Placement in the Lee of a Mountain Ridge A Wind Tunnel Study

Environmental Sciences Research Lab, Research Triangle Park, NC

Sep 76

TECHNICAL REPORT DATA
(Please read Instructions on the reverse before completing)

1. REPORT NO.	2.	3. RECIPIENT'S ACCESSION NO.
EPA-600/4-76-047		

4. TITLE AND SUBTITLE
STACK PLACEMENT IN THE LEE OF A MOUNTAIN RIDGE
A Wind Tunnel Study

5. REPORT DATE
September 1976

6. PERFORMING ORGANIZATION CODE

7. AUTHOR(S)
Alan H. Huber, William H. Snyder*,
Roger S. Thompson, and Robert E. Lawson, Jr.

8. PERFORMING ORGANIZATION REPORT NO.
Fluid Modeling Report No. 2

9. PERFORMING ORGANIZATION NAME AND ADDRESS
Environmental Sciences Research Laboratory
Office of Research and Development
U.S. Environmental Protection Agency
Research Triangle Park, N.C. 27711

10. PROGRAM ELEMENT NO.
1AA603

11. CONTRACT/GRANT NO.

12. SPONSORING AGENCY NAME AND ADDRESS
Environmental Sciences Research Laboratory
Office of Research and Development
U.S. Environmental Protection Agency
Research Triangle Park, N.C. 27711

13. TYPE OF REPORT AND PERIOD COVERED
In-house 1/75 - 6/75

14. SPONSORING AGENCY CODE
EPA-ORD

15. SUPPLEMENTARY NOTES
* On assignment from the National Oceanic and Atmospheric Administration.

16. ABSTRACT: An investigation of the highly turbulent region in the lee of a two-dimensional mountain ridge was carried out in the Meteorological Wind Tunnel of the U.S. EPA's Fluid Modeling Facility. This highly turbulent region was found to consist of a large semi-permanent eddy. Smoke visualization and hot film anemometry measurements showed that the cavity size and shape are minimally affected by the thickness and turbulence intensity of the approach boundary layer flow. In addition, the cavity size and shape were not found to be affected by the detailed shape of the ridge, but were strongly dependent upon the upwind terrain and the gross features (angles) of the downslope.

A stack was positioned to emit an air-methane mixture into the cavity in the lee of the ridge. Longitudinal, lateral and vertical concentration profiles were taken. A tall stack placed to emit into the upper portion of the cavity resulted in higher ground level concentrations near the downwind end of the cavity than did a shorter stack. However, the maximum concentrations measured were found to occur near the bases of the shorter stacks.

The cavity region leeward of the model ridge was found to be highly turbulent with significant plume downwash. For similar real-atmosphere situations, it would be good engineering practice to avoid placement of any significant source within the expected cavity region. Application of the "2 1/2 times rule" for stack construction would be sufficient to avoid the highly turbulent region of the cavity proper.

17. KEY WORDS AND DOCUMENT ANALYSIS

a. DESCRIPTORS	b. IDENTIFIERS/OPEN ENDED TERMS	c. COSATI Field/Group
Air pollution		13B
Wind tunnel		14B
Boundary layer		20D
Atmospheric diffusion		04A
Mountain ridges		08F
Chimneys		13M
Downwash		20D

18. DISTRIBUTION STATEMENT	19. SECURITY CLASS *(This Report)*	21. NO. OF PAGES
RELEASE TO PUBLIC	UNCLASSIFIED	55
	20. SECURITY CLASS *(This page)*	22. PRICE
	UNCLASSIFIED	$4.50

EPA Form 2220-1 (9-73)

PB 259 877

REPRODUCED BY
NATIONAL TECHNICAL
INFORMATION SERVICE
U. S. DEPARTMENT OF COMMERCE
SPRINGFIELD, VA. 22161

EPA-600/4-76-047
September 1976

STACK PLACEMENT IN THE LEE OF A MOUNTAIN RIDGE

A Wind Tunnel Study

by

Alan H. Huber
Monitoring and Data Analysis Division
Office of Air Quality Planning and Standards
Research Triangle Park, N.C. 27711

William H. Snyder
and
Roger S. Thompson
Meteorology and Assessment Division
Environmental Sciences Research Laboratory
Research Triangle Park, N.C. 27711

Robert E. Lawson, Jr.
Northrop Services, Inc.
Research Triangle Park, N.C. 27711

ENVIRONMENTAL SCIENCES RESEARCH LABORATORY
OFFICE OF RESEARCH AND DEVELOPMENT
U.S. ENVIRONMENTAL PROTECTION AGENCY
RESEARCH TRIANGLE PARK, N.C. 27711

DISCLAIMER

This report has been reviewed by the Environmental Sciences Research Laboratory, U.S. Environmental Protection Agency, and approved for publication. Mention of trade names or commercial products does not constitute endorsement or recommendation for use.

ABSTRACT

In a wind tunnel study, the highly turbulent region in the lee of a two-dimensional mountain ridge was found to consist of a large semipermanent eddy that was caused by the separation of the main flow at the apex of the ridge. General circulation of this eddy was in the main flow direction along the upper edge, opposite the main flow direction along the ground surface, and up the slope along the leeward ridge surface. Smoke visualization and hot film anemometry measurements showed that the cavity size and shape were minimally affected by the thickness and turbulence intensity of the approach boundary layer flow. In addition, the cavity size and shape were not found to be affected by the detailed shape of the ridge, but were strongly dependent upon the upwind terrain and the gross topographic features (angles) of the downslope. The largest cavity was found to extend to two ridge heights in the vertical and to ten ridge heights downwind.

A model stack was positioned to emit an air-methane mixture into the cavity in the lee of the ridge. Longitudinal, lateral, and vertical concentration profiles were taken. A tall stack placed to emit the test mixture into the upper portion of the cavity produced higher ground level concentrations near the downwind end of the cavity than did a shorter stack. The maximum measured concentrations, however, were found to occur near the bases of the shorter stacks.

The cavity region leeward of the model ridge was found to be highly turbulent with significant plume downwash. For similar real-atmosphere situations, it would be good engineering practice to avoid placement of any significant source within the expected cavity region. Application of the "2 1/2 times rule" (with respect to the ridge height) for stack construction would be sufficient to avoid the highly turbulent region of the cavity proper.

CONTENTS

Abstract ---------- iii

Figures ---------- vi

Symbols ---------- ix

1. Introduction ---------- 1

2. Conclusions and Recommendations ---------- 3

3. Review of Literature ---------- 4

4. Design of the Experiment ---------- 9

5. Experimental Details and Equipment ---------- 11

6. Results ---------- 17

6.1 Phase I: Envelope and Cavity Visualization Results for the 30 cm Gaussian Ridge and 30 cm Triangular Ridge ------- 17

6.2 Phase I: Mean Velocity and Turbulence Intensity Measurements for the 30 cm Gaussian Ridge and 30 cm Triangular Ridge ---------- 17

6.3 Phase II: Concentration Measurements for a Stack Placed in the Lee of the 30 cm Gaussian Ridge ---------- 21

6.4 Phase III: Cavity and Envelope Measurements in the Lee of the 15 cm Gaussian Ridge ---------- 35

7. Discussion and Summary ---------- 39

References ---------- 42

Preceding page blank

FIGURES

Number		Page
1	Diagrammatic sketch of envelope and cavity regions behind a two-dimensional ridge	2
2	Cavities behind obstacles (boundary layer thicknesses and cavity dimensions are given as multiples of the obstacle or step height)	7
3	Diagrammatic sketch of wind tunnel with vortex generators and roughness slats in place	12
4	Mean velocity and turbulence intensity profiles 5.5 m downstream from vortex generator trailing edge	12
5	End views of two-dimensional ridges	13
6	Phase III ridge configurations	16
7	Envelope size in lee of 30.5-cm Gaussian ridge	18
8	Cavity size in lee of 30.5-cm Gaussian ridge	18
9	Envelope size in lee of 30.5-cm triangular ridge	19
10	Cavity size in lee of 30.5-cm triangular ridge	19
11	Smoke envelope in lee of (A) 30-cm Gaussian ridge and (B) 30-cm triangular ridge (The strut supporting the smoke tube is laterally displaced from the smoke filled region.)	20
12	Mean velocity and turbulence intensity profiles for 30.5-cm Gaussian ridge (separation not forced), U_∞ = 3.05 m/sec	22
13	Mean velocity and turbulence intensity profiles for 30.5-cm Gaussian ridge (separation not forced), U_∞ = 9.15 m/sec	22
14	Mean velocity and turbulence intensity profiles for the 30.5-cm Gaussian ridge, U_∞ = 3.05 m/sec	23
15	Mean velocity and turbulence intensity profiles for the 30.5-cm Gaussian ridge, U_∞ = 9.15 m/sec	23

16 Mean velocity and turbulence intensity profiles for the 30.5-cm triangular ridge, U_∞ = 3.05 m/sec 24

17 Mean velocity and turbulence intensity profiles for the 30.5-cm triangular ridge, U_∞ = 9.15 m/sec 24

18 Ground level concentration measurements with sampling probe fixed near base (x/H = 3 from ridge center, z/H = 0) of 30.5-cm Gaussian ridge (Stack was placed at four downwind locations and its height was varied 25

19 Longitudinal ground level concentration profiles downwind from stack placed at base (x/H = 2.7 from center) of 30.5-cm Gaussian ridge 26

20 Vertical concentration profiles from stack placed at base (x/H = 2.7 from center) of 30.5-cm Gaussian ridge, H_s/H = 0.5 28

21 Smoke visualization with 0.5 H stack placed at base of 30-cm Gaussian ridge (x/H = 2.7 from ridge center) 29

22 Lateral concentration profiles from stack placed at base (x/H = 2.7 from center) of 30.5-cm Gaussian ridge, x/H = 1.25, H_s/H = 0.5 30

23 Lateral concentration profile from stack placed at base (x/H = 2.7 from center) of 30.5-cm Gaussian ridge, x/H = 2.25, H_s/H = 0.5 30

24 Lateral concentration profiles from stack placed at base (x/H = 2.7 from center) of 30.5-cm Gaussian ridge, x/H = 4.75, H_s/H = 0.5 31

25 Elevated longitudinal concentration profile downwind from stack placed at base (x/H = 2.7 from center) of 30.5-cm Gaussian ridge, H_s/H = 0.5 31

26 Vertical concentration profiles from stack placed at base (x/H = 2.7 from center) of 30.5-cm Gaussian ridge H_s/H = 1.5 32

27 Smoke visualization with 1.5 H stack placed at base of 30-cm Gaussian ridge (x/H = 2.7 from ridge center) 33

28 Lateral concentration profile from stack placed at base (x/H = 2.7 from center) of 30.5-cm Gaussian ridge, x/H = 1.25, H_s/H = 1.5 34

29 Lateral ground level concentration profiles from stack placed at base (x/H = 2.7 from center) of 30.5-cm Gaussian ridge, z/H = 0, H_s/H = 1.5 34

30 Envelope and cavity size in lee of 15.2-cm Gaussian ridge (60-cm simulated boundary layer) 35

31 Mean velocity profiles above center of 15.2-cm Gaussian ridge 36

32 Envelope and cavity in lee of 15.2-cm Gaussian ridge (15-cm natural boundary layer) 37

33 Envelope and cavity size in lee of 15.2-cm Gaussian ridge (15-cm natural boundary layer with raised plane approach) 37

34 Envelope and cavity size in lee of 15.2-cm Gaussian ridge (60-cm simulated boundary layer with raised plane approach) 38

35 Envelope and cavity size in lee of 15° sloping plane (60-cm simulated boundary layer with raised plane approach) 38

SYMBOLS

L	characteristic width of ridge
H	height of obstruction (ridge, etc.)
H_s	height of stack
D	inside diameter of stack
δ	boundary layer thickness
U	mean wind speed (a function of elevation)
U_s	wind speed at top of stack
U_∞	free-stream wind speed
$\sqrt{\overline{u'^2}}$	root-mean-square of longitudinal velocity fluctuations
W_s	stack effluent speed
ν	kinematic viscosity of air
Re	Reynolds number
Q	stack emission rate
C_s	stack gas concentration
χ	concentration (a function of location)
C	concentration expressed as the percent of stack gas concentration
M	used as subscript to denote measurements under a model scale situation
F	used as subscript to denote measurements under full scale field situation
R	radius of curvature
x	longitudinal distance (origin as specified)
y	lateral distance from center of tunnel
z	vertical distance from floor of tunnel

SECTION 1

INTRODUCTION

Aerodynamic effects induced by local terrain features can have a major influence upon the dispersion of locally emitted effluents. Even when the best demonstrated control technology is applied, pollutant concentrations are usually at levels far in excess of ambient air quality standards as the plume leaves the stack. In addition, the plume may frequently be entrained in the turbulent eddies created by air flow over local terrain features and be brought to the ground before the pollutant concentrations are reduced to levels below ambient air quality standards. Thus, it is important that those persons responsible for stack design and location have an adequate understanding of such adverse aerodynamic effects.

For neutral (neutrally stable) atmospheric flow, aerodynamic effects evolve from interacting frictional forces and pressure gradients induced by local surface roughness and terrain features. Adverse effects exist when surface friction and pressure gradients combine to retard the surface layer flow enough to produce separation of the boundary layer. Separation in a neutral flow generally occurs near the apex of the terrain feature -- resulting in a stagnation region on the leeward side, often referred to as a "cavity". At the point of separation, the main stream of flow is vertically raised, causing a stagnation region (cavity) to develop below. Mean velocities in this cavity are reduced and the flow is highly turbulent. The flow reattaches itself somewhere downstream of the obstacle. In the region of reattachment, a portion of the flow is deflected upstream, forming a zone of recirculation. The dividing "streamline" that separates the recirculating flow from the main stream encloses the cavity, as shown in Figure 1. The wake, defined as that region of the flow field that is disturbed by the obstacle, can extend very far downwind. (The "envelope" is the upper boundary of the wake.) Far enough downwind, of course, the flow readjusts itself to a boundary layer appropriate to local surface roughness.

For a moderately stable atmospheric flow, the separation point generally shifts to a position on the leeward side, which results in a smaller cavity. For highly stable flows, separation may disappear entirely, or other phenomena, such as lee waves and rotors, may be found. These phenomena also have the potential to affect plume dispersion. Unstable flows, on the other hand, can either enhance or delay separation.

Terrain features that most adversely affect the flow are two-dimensional in nature. Lateral air motion around a hill results in a smaller cavity size than would be observed for a two-dimensional ridge. A study of neutral flow with separation occurring at the apex of a two-dimensional mountain ridge would, therefore, best demonstrate the extent to which stagnation regions can

influence the dispersion of locally emitted effluents.

The objective of this study, conducted at the U.S. Environmental Protection Agency's Fluid Modeling Facility, was to simulate neutral atmospheric flow over a two-dimensional mountain ridge and to examine the effects of the ridge on stack plume dispersal and resultant ground level pollutant concentrations. The ultimate goal was to develop guidance for determining "good engineering practice" when selecting the site for a stack.

There were three major phases to this study. In the first phase, velocity and cavity size measurements were made in order to demonstrate that the basic flow structure is independent of the detailed shape of the ridge (Gaussian or triangular). In the second phase, the concentration field resulting from a source placed within the cavity was delineated. In the third phase, the effect of variations in the approach flow on the cavity size and shape was examined. The results presented in this report should enable the reader to better understand the atmospheric flow structure so that good engineering practice can be used in locating stacks or determining necessary stack heights, and that "order of magnitude" ground level concentrations can be predicted in the event the stack emits into the cavity region.

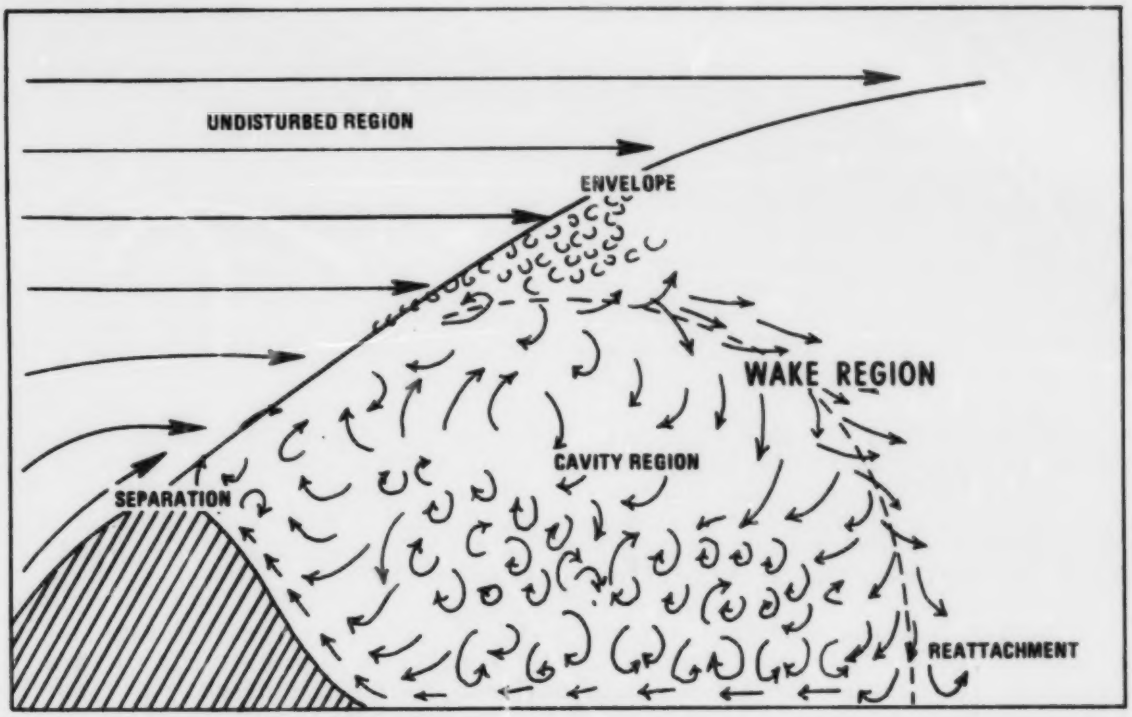

Figure 1. Diagrammatic sketch of envelope and cavity regions behind a two-dimensional ridge.

SECTION 2

CONCLUSION AND RECOMMENDATIONS

The cavity region leeward of the model ridge was found to be highly turbulent with significant plume downwash. For similar real-atmosphere situations, it would be good engineering practice to avoid placing any significant source within the expected cavity region. Application of the "2 1/2 times rule" with respect to the ridge height would be sufficient to avoid the highly turbulent region of the cavity proper. Although the maximum depth of the cavity was found to be 2 H, some margin of safety is well advised because strong downdrafting occurs in the upper regions of the cavity. The maximum horizontal extent of the cavity was found to be 10 H. Because the turbulence intensity and thus the plume dispersion are increased in the envelope above the cavity, part of a plume emitted above a cavity can, in only a short distance, spread downward and thus become entrained within the cavity.

The concentration measurements from the stack placed in the cavity region were helpful in providing a description of the effects that the ridge had on stack plume dispersal. For the short stacks (0.5 H and 1 H stack heights), the highest ground level concentrations were found at a position very near the stack. For the 1.5 H stack, the highest ground level concentrations occurred significantly further downwind of the stack. From these results, it is evident that instead of the strong immediate downwash, which occurred for the shorter stack, the taller stack emissions are caught in the outer recirculation region within the cavity. Maximum ground level concentrations, which did occur within the cavity region, were found to be of the order 0.05 - 0.1 percent of the stack effluent concentration. These concentrations are undoubtedly significantly higher than would occur in the absence of the mountain lee effects examined in this study. If further concentration mappings were made, having a greater variety of stack locations within the cavity and a greater variety of stack emission characteristics, a general guideline for estimating ground level concentrations could be developed. This additional delineation would be quite useful for those circumstances that may arise when building a stack 2 1/2 times the ridge height would be impractical.

Downwind of the cavity region the turbulence intensity was still significantly greater than that found in the undisturbed flow. Further studies of the behavior of plumes from sources placed downwind of the cavity region are needed to characterize dispersion there.

SECTION 3

LITERATURE REVIEW

The general engineering "rule of thumb" for avoiding plume downwash in the lee of a ridge is to keep the height of the stack 2 1/2 times the height of the ridge. According to Sutton (1960), the rule was probably derived by Sir David Brunt from a study on the height of atmospheric disturbances over a long ridge in connection with a British airship disaster investigation.

The downwind range of the strong downwash region (cavity) depends on the general form of the obstruction being considered. Flow around a cube, for example, was found to form a cavity extending 2 barrier heights downwind (Evans, 1957). When the width perpendicular to the wind direction was increased to 8 heights, the cavity length increased to 5 heights downwind, but the vertical extent of the cavity region increased only slightly. The greatest extent of the cavity region may, therefore, be expected to occur in the lee of the two-dimensional ridge.

The ASME Guide (1968) reported that the plume from a stack placed in the cavity leeward of a valley ridge became thoroughly diffused before passing downwind to the wake region where the flow was in the direction of the upper wind. The plume was distributed vertically throughout much of the valley depth. Briggs (1969) reported that a terrain feature can affect a plume in much the same manner as a building, which causes high concentrations of the effluent to be brought to the ground. A brief discussion of effects induced by terrain was presented by Strom (1968). The turbulent region on the leeward side was described as a region in which the plume can be brought quickly to the ground, diffused over a wide area, or, in extreme cases, transported up the hill because of a large standing eddy. This turbulent region was reported to extend to elevations well above the hill top, depending on the abruptness of the windward side.

A detailed discussion of separation and wake formation was presented in Halitsky (1968). Most of the experimental results reported, however, related to three dimensional obstructions. Interestingly, he raised the point that: "no wind-tunnel measurements of concentrations in plumes that have descended into the wake appear in the literature, owing partly to the limited number of facilities available for this type of test and partly to the policy of industrial sponsors not to release such information." The interest in application of fluid models to the study of air pollution has since increased, and therefore the number of facilities and reports published in the literature has been increasing.

According to Scorer (1955), the separation point is stationary when there is a salient edge at the top of a hill or ridge, and he cites numerous, but

limited, field studies relating to the zone of recirculation and instances of intense mixing and general downdrafting in the leeward regions of ridges. Details are insufficient to draw firm conclusions relating to formation of separated flows.

The general features of flow over a ridge were treated theoretically and experimentally by Buettner (1964). A ridge station was constructed on the lee side of the Ipsut Pass area of Mount Rainier National Park in Washington as part of a study of the effect of terrain obstacles on the fallout of particulate matter through the atmosphere. Tracer particles of zinc sulfide were released and collected. Data were collected for 5 days during which the airflow approach was perpendicular to the ridge. During the period of experimental set-up, only light-moderate winds were observed. The most common wind field occurrence was reported as a "vortex sheet flow" with the airstream separating from the ridge top and forming a wake zone in the lee of the ridge. For this flow, the wind field was constant above and zero below a plane representing the wake zone. Only a small amount of particulate penetrated down through the horizontal vortex sheet. A contaminant released in the calm zone was reported to meander in an unpredictable manner. Previously, a lee eddy with the main airstream moving first horizontally away from the ridge, then down, and then up again close to the valley bottom was visually observed. At this site, such a flow pattern was believed to exist only for strong winds. Laminar flow complicated by thermal winds was reported to occur when stable settled conditions prevail and the gradient wind at ridge level was less than 6 knots (3.1 meters per second).

Some characteristics of wind field modification by natural obstructions were reported by Gloyne (1965). An eddy flow 2 barrier heights in vertical extent and 10 to 15 barrier heights in horizontal extent to the leeward side of a "near solid" barrier was diagrammed. At ground level, the region of disturbed flow extended to about 30 barrier heights. Downwind of a steeply sloped, wooded hill with a wind blowing at right angles to its length, the disturbed flow was reported to also extend downwind to about 30 times its height. Additional discussions relevant to wind modifications were also presented, and the point was made that each case must be assessed separately. Slope angle and thermal stability and wind speed were influential factors in determining the extent of terrain-induced disturbances

Pooler and Niemeyer (1970) presented, as part of a study evaluating dispersion from tall stacks, several situations in which unexpectedly high ground level concentrations could be associated with mountain lee effects. On days with neutral flow, the plume from a stack located 13 ridge heights downwind from a 450-m ridge was carried down to ground level within a very short distance. This phenomenon could well be a result of the strong downwash that occurs near the leeward edge of a standing eddy.

Corby (1954) reviewed the work of J. Forchtgott, who gathered about 35 different sets of observations involving five different mountain ridges located in Bohemia. Mountain airflow was classified into four main types: (1.) undisturbed streaming, (2.) standing eddy streaming, (3.) wave streaming, and (4.) rotor streaming. The case of standing eddy streaming

corresponded to the situation of boundary layer separation at the ridge apex with cavity formation in the lee. This type of flow was reported to have been observed frequently. Forchtgott implied that this situation was predominant under moderate wind speed and wind shear conditions. Even for the cases with smooth waves above, some form of turbulent wake was found in the lee of the ridge.

A World Meteorological Organization technical note (1967) arrived at a similar conclusion. Over rugged terrain, whether the flow aloft was smooth or otherwise, it usually rested on a turbulent wake. Although little descriptive detail of such regions was presented in the report, many photographs showed the wave structures above the wakes, as revealed by cloud formations.

The results of a number of balloon releases made in two valleys in Vermont were reported by Davidson (1963). Balloon releases were made at several positions along the sides of ridges that had approximately 20° slopes. Balloon paths were determined using theodolites. The limited results could not be used to confirm a point of separation or the extent of a leeward cavity region. The extreme turbulence generated in the lee of the ridges, however, appeared to be dissipated at most elevations at a distance of 4 to 6 heights downwind.

Halitsky, et al. (1966) reported comparisons between their wind tunnel model results and Davidson's (1963) field observations in the lee of Green Peak, Vermont. Best agreement resulted for the higher model wind speeds suggesting that tests of this type be run with a minimum ridge height Reynolds number of 1×10^5. The field observations of a cavity and wake flow generally fitted the model test results.

An extensive literature review relating to both field and fluid modeling studies and a discussion as to how mountainous terrain can alter atmospheric airflow were offered by Orgill, et al. (1971). The authors reported that, for neutral airflow over a mountain, a large semipermanent eddy occurs on the lee side. An area in the central Rocky Mountains of Colorado was chosen for a field and laboratory study of transport and dispersion over irregular terrain. Two different atmospheric conditions were simulated: the thermal stability used in the wind tunnel model was near-neutral in the lower levels and stable in the upper levels for one case and totally neutral throughout for the other case. Field data yielded information on the mean velocity and dispersion characterisitics over the local terrain. Totally neutral atmospheric stability conditions were observed on only one day. No specific information as to where and when boundary layer separation occurs or the size or shape of the cavity region in the lee of ridges was reported in either the field or laboratory study results. The purpose of the report was to generalize on flow patterns in complex terrain on a much larger scale.

Some discussion of fluid modeling studies on the flow behind regular-shaped obstacles is relevant. Bradshaw and Wong (1972) compared the cavity sizes found by several investigators. This comparison plus some recent additions are shown in Figure 2. In the figure, the cavity size and boundary layer depth are given in terms of the obstacle height, H.

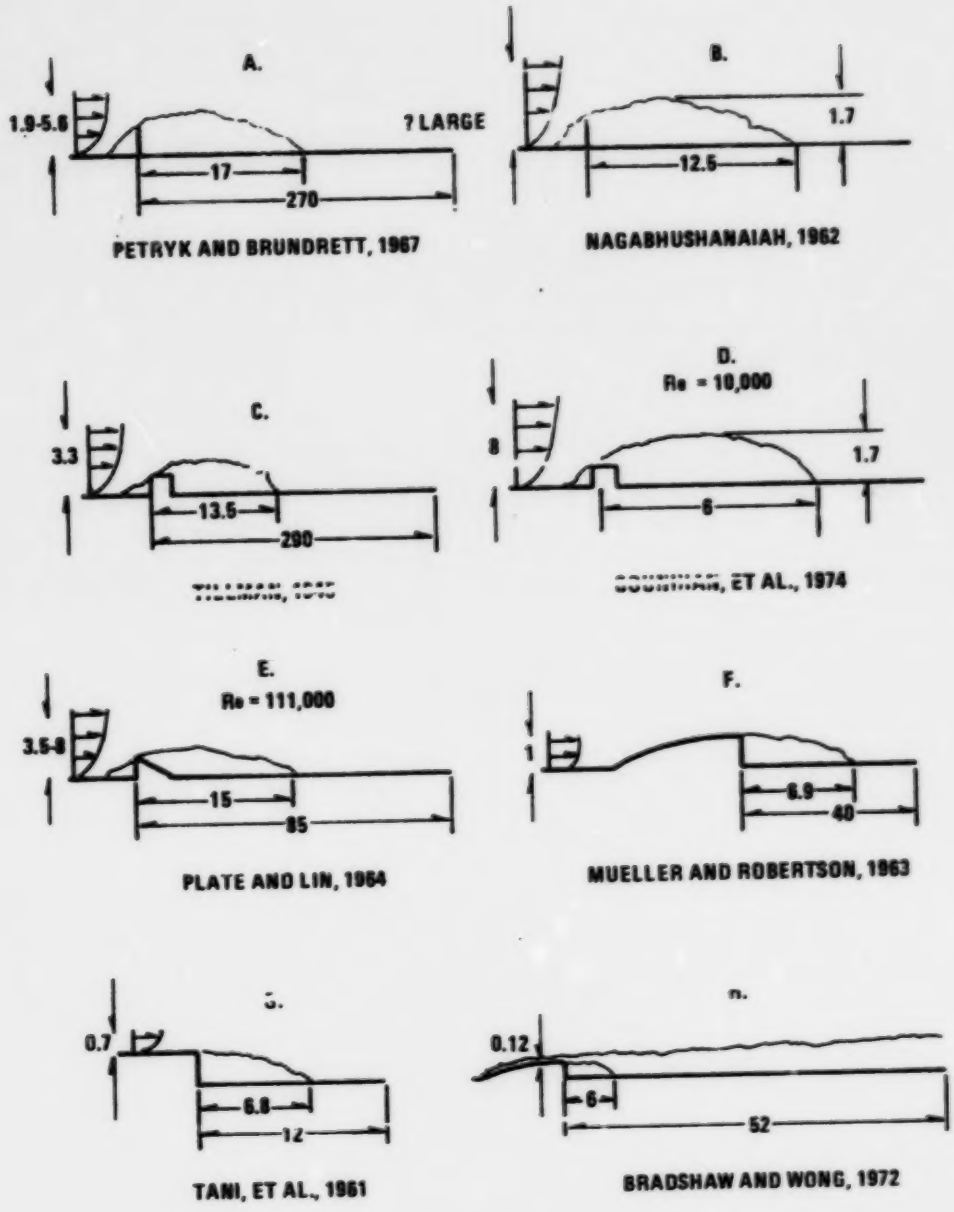

Figure 2. Cavities behind obstacles (boundary layer thickness and cavity dimensions are given as multiples of the obstacle or step height).

Diffusion into the boundary layer downstream from a two-dimensional sinusoidal ridge was examined by Plate and Sheih (1965). A continuous point source of helium was placed at the crest of the model. The diffusion characteristics were found not to differ from the case of a smooth flat plate when the boundary layer did not separate from the model. Both plume height and width were found to increase significantly in the immediate downwind neighborhood of the model when separation did occur. Further downwind, however, the rate of growth naturally decreased and became similar to that in an undisturbed boundary layer. The size of the cavity in the lee of this model was not shown.

Diffusion from a ground line source upwind from a fence was examined by Plate (1967). Downstream from the reattachment point, the concentration profile was found to follow a similarity law whose shape corresponded to that in an undisturbed boundary layer. No measurements of concentrations inside the cavity region were included.

The review of published field studies presented here strongly supports the assertion that, on the leeward side of a mountain ridge, a recirculating flow region with strong downwash and dispersion characteristics can exist. However, information that could define the point of separation and the size and extent of the cavity was not found. The point of separation appears to be very much a function of mean flow speed and direction, atmospheric stability, both the downslope and upslope angle of the ridge sides, and the location of the ridge with respect to surrounding terrain.

For a particular situation, the greatest size of the cavity will take place when separation occurs at the ridge apex. Both field results and fluid modeling results confirm the natural expectation that the more obtrusive the ridge, the larger the cavity region. Obstructions with salient features should exhibit definite separation at their edges under all atmospheric conditions. The size of the cavity region is greatest for isolated ridges with steep sloping sides. Stable atmospheric conditions act to restrict the size and extent of the cavity region.

SECTION 4

DESIGN OF EXPERIMENT

To ensure that the flow in the model accurately simulates that in the atmosphere, it is necessary to meet certain similarity criteria. Various nondimensional parameters that characterize the flow in the atmosphere -- including the Rossby number, the Reynold number, the Froude number, the Richardson number, etc. -- must be matched in the model. Because this study is concerned only with neutral atmospheric flows involving nonbuoyant effluents and relatively small scales, the Richardson, Froude and Rossby numbers may be ignored (Snyder, 1972). The remaining parameters of significance are as follows:

$$\frac{L}{H}, \frac{H_s}{H}, \frac{D}{H}, \frac{\delta}{H}, \frac{U}{U_\infty}, \frac{\sqrt{\overline{u'^2}}}{U}, \frac{W_s}{U_s}, \frac{U_\infty H}{\nu}, \text{ and } \frac{W_s D}{\nu}.$$

The first three of these parameters (length ratios) are easily matched by constructing a scale model, but because no particular field situation was modeled, idealized ridge shapes and representative values were chosen. The next three parameters characterize the boundary layer approaching the ridge. Two different boundary layers were used. One was a thick, simulated atmospheric boundary layer; the other was the natural (thin) boundary layer developed over the smooth wind tunnel floor.

The effluent speed to wind speed ratio was maintained at 3:2 in all tests. This value is the minimum necessary to avoid downwash in the immediate lee of the stack itself (Sherlock and Stalker, 1940). Under these conditions (minimum effluent speed to wind speed ratio and zero buoyancy), the effective stack height is essentially the same as the physical stack height. These conditions were chosen in order to be able to equate the effective stack height in an undisturbed flow to the physical stack height. Plume rise or downwash from the model stack placed in the lee of the ridge are therefore associated with induced disturbances.

The last two parameters are the ridge Reynolds number ($Re_H = U_\infty H/\nu$) and the effluent Reynolds number ($Re_D = W_s D/\nu$). For exact similarity, the model ridge Reynolds number must equal the actual ridge Reynolds number. This is not possible for the model scale used and, fortunately, is not necessary (Snyder, 1972) because at sufficiently large Reynolds numbers, the pattern of flow becomes independent of Reynolds number. For a mountain ridge having a salient feature, near the top of the ridge, the boundary layer may be expected to separate near its apex (Scorer, 1968, p. 108). For a ridge not having a salient feature, the separation point may fluctuate in position,

and may even occur on the downwind side of the ridge, which would result in a smaller cavity. In the field, the ridge Reynolds number based on a ridge height greater than 75 m and free-stream wind speed greater than 3.0 m/sec is greater than 1×10^7. For these very large Reynolds numbers, separation is certain to occur at or slightly windward of the apex, even for a ridge with a smooth rounded top (Scorer, 1968, p. 113). The Reynolds number for the model mountain ridges lies between 1×10^4 and 1×10^5, which is much smaller than the full scale Reynolds number. At these smaller Reynolds numbers, the location of the separation point is affected by the Reynolds number. If the point of separation on the model occurs at its apex, however, similarity of the two flow patterns should result. Hence, a small trip (1.25 cm-high slat, see Figure 11 A) was placed at the apex of the rounded ridge in order to ensure separation at that point.

The plume behavior is independent of the effluent Reynolds number provided the flow is fully turbulent at the stack exit. The value of 2000 is well-established for the maintenance of turbulent flow in a pipe. Because the effluent flow appeared to be laminar as it was ejected from the stack, internally serrated washers were placed inside the stack to ensure fully turbulent flow at the exit (Lin et al., 1974).

Concentrations measured in the model can also be related to those that would be measured in the field. For most situations, the stack emissions may be assumed to behave as point sources. The stack gas concentration, C_s (gram per cubic meter), is related to the stack emission rate, Q (gram per second), by

$$Q = C_s \left(\frac{\pi}{4} D^2\right) W_s. \tag{1}$$

The field concentration, χ_F, is linearly related to the model concentration, χ_M; to the emission ratio, Q_M/Q_M ; and to the dilution ratio, $U_M H_M^2 / U_F H_F^2$. These basic relations result in the expression

$$\chi_F = \chi_M \left(Q_F/Q_M\right) \left(U_M/U_F\right) \left(H_M/H_F\right)^2$$

or

$$(\chi/C_s)_F = [(\chi/C_s)_M] [(W_s/U_s)_F/(W_s/U_s)_M] [(D/H)_F^2/(D/H)_M^2]. \tag{2}$$

With strict matching (identical effluent speed to wind speed ratios and stack diameter to ridge height ratios), the model concentration ratios are equal to the field concentration ratios, $(\chi/C_s)_M = (\chi/C_s)_F$. Relaxation of the requirements for strict matching of the stack diameter to ridge height ratios and effluent to wind speed ratios permits a wider applicability of the concentration measurements, provided the plume paths are similar.

SECTION 5

EXPERIMENTAL DETAILS AND EQUIPMENT

The experiments were carried out in the meteorological wind tunnel of EPA's Fluid Modeling Facility. The wind tunnel has a test section measuring 3.7 m x 2.1 m x 18.3 m, and the flow speed within the wind tunnel can be controlled between 0.3 and 10.0 m/sec. Further details of the wind tunnel can be obtained from Snyder, et al., (1976).

In performing fluid modeling studies, it is important to simulate the atmospheric boundary layer. The natural wind tunnel boundary layer that develops over the smooth tunnel floor is generally too thin and possesses insufficient turbulence intensity for accurate simulation. A thick, turbulent boundary layer was simulated by the method of Counihan (1969), who used a castellated barrier placed at the test section entrance slightly upstream from semielliptical, wedge shaped vortex generators. Counihan used three-dimensional blocks downwind of the generators to maintain the boundary layer. In the present study, two-dimensional roughness slats were found to be sufficient to maintain the boundary layer in equilibrium. These experiments used a 15-cm-high barrier, 60-cm-high generators, and 7 m of 0.635 cm x 1.43 cm slats placed across the floor perpendicular to the wind direction with centers placed 15.24 cm apart (Figure 3). The ridge was placed just downstream of the last roughness slat. A 60-cm-thick boundary layer with an approximate one-seventh power law mean velocity profile was measured in a separate study 5.5 m downstream from the vortex generator trailing edge (Figure 4). The one-seventh profile is generally accepted to represent neutral atmospheric flow over relatively smooth terrain (open country, grassland -- Davenport, 1963). The vortex generator-roughness element combination described above also produces a suitable turbulence intensity profile representative of atmospheric flow over relatively smooth terrain (Figure 4).

Three model ridges were constructed and are shown in Figure 5. One ridge was triangular in shape with a 30.5-cm-high apex and sloping sides of 30°; the other two had sides with idealized shapes. The latter two ridges were symmetrical about a centerline, each side of which could be divided into three sections. The center section had a constant slope of 30°, and the upper and lower sections were convex and concave outward, respectively. This model shape appears to be very close to a Gaussian probability distribution and is referred to throughout this report as the Gaussian model ridge in order to distinguish it from the triangular model ridge. The two similar Gaussian ridges have apexes of 30.5 cm and 15.2 cm in height, respectively. The three models will be referred to in the remainder of this report as the 30-cm triangular ridge, the 30-cm Gaussian ridge, and the 15-cm Gaussian ridge.

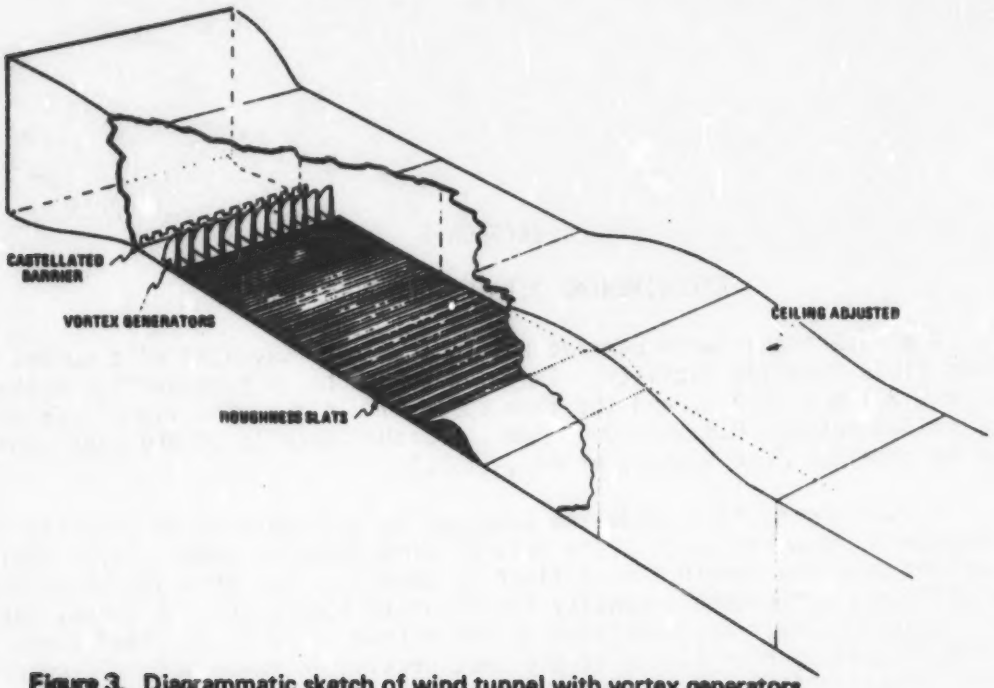

Figure 3. Diagrammatic sketch of wind tunnel with vortex generators and roughness slats in place.

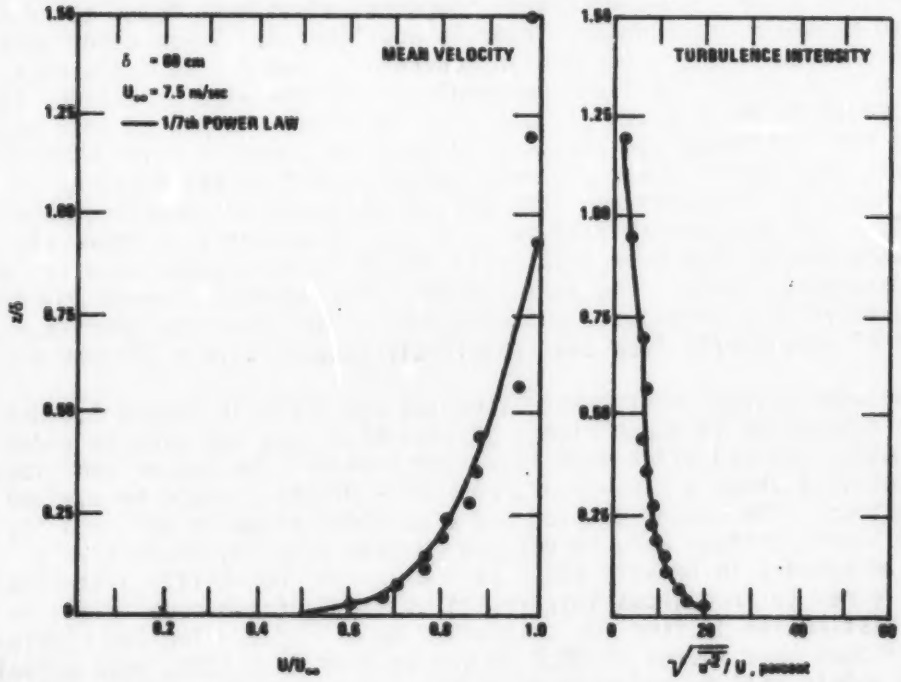

Figure 4. Mean velocity and turbulence intensity profiles 5.5 m downstream from vortex generator trailing edge.

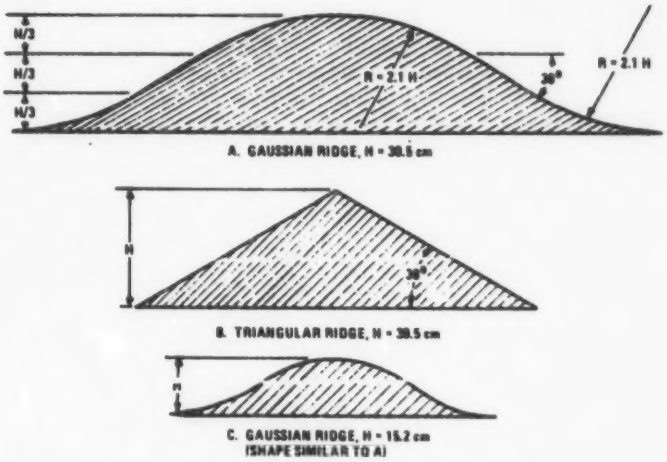

Figure 5. End views of two-dimensional ridges.

In Phase I of this study, the primary goal was to examine whether the flow structure is independent of the detailed shape of the ridge. Smoke tests were made to define the shapes of the cavities and envelopes, and hot film measurements were made to compare the flow fields above and downwind of the 30-cm Gaussian ridge and the 30-cm triangular ridge. The approach flow for all tests was that of the 60-cm simulated boundary layer.

For the 30-cm Gaussian ridge, smoke visualization indicated the cavity region to be dependent on the free-stream velocity. A 1.25-cm-high slat was placed along the apex of the ridge in order to trip the flow and induce separation at that point. The triangular ridge exhibited flow separation at its apex without the addition of a trip.

Further experimentation with the tripped, 30-cm Gaussian-shaped ridge and the triangular ridge indicated that the cavity region on the leeward side was independent of free-stream velocity (Section 6.1). This was determined through smoke visualization. At various downstream positions, a smoke source was raised in the vertical to a point where no smoke could be seen recirculating back to the base of the hill. These vertical positions were used to define the boundary shape of the leeward cavity. The "envelope" was determined from observations of the maximum vertical spread of smoke emitted within the cavity region.

For mean velocity and turbulence intensity profiles, a hot film sensor and anemometer were used. A Thermo-Systems Inc. Model 1054 A anemometer was used in conjuction with the company's Model 1210-20 hot film probe. The resulting measurements for both the 30-cm tripped Gaussian ridge and the triangular ridge were quite similar (Section 6.2). Because of the similarity, only the tripped Gaussian ridge was used in further analyses (Phases II and III).

In Phase II, the goal was to map the concentration field resulting from

a stack emitting into the cavity region. The approach flow was the 60-cm simulated boundary layer. A stack was placed in the center of the tunnel at the leeward base edge of the tripped, 30-cm Gaussian ridge (2.7 H downwind of the ridge center). The stack inside diameter (ID) was 0.89 cm, and the outside diameter (OD) at the stack top was 1.1 cm. If the model ridge were scaled to a 150-m mountain ridge, the stack would represent a 4.5-m ID stack with a 1-m wall thickness. Although not crucial, these scales correspond reasonably well to representative field situations. Longitudinal (x, downwind from center of ridge), lateral (y, from center of tunnel), and vertical (z, from floor of tunnel) concentration profiles were taken for stack heights of 0.5 H and 1.5 H and a free-stream velocity of 3.05 m/sec.

An air-methane mixture was ejected from the stack as a tracer gas. This effluent simulated a neutrally buoyant plume because the amount of methane in the gas mixture was only 1 percent and the stack gas temperature was equal to the ambient air temperature. The stack exit velocity was controlled to permit an effluent to wind speed ratio of 3:2. This ratio has general acceptance as a "rule of thumb" for avoiding stack downwash. With the stack placed in the free-stream flow, a minimal plume rise without any downwash was achieved. The above stack conditions were selected so that all plume rise and downwash could be associated with effects from the mountain ridge. The stack exit velocity, W_s, was 4.57 m/sec, which made the stack Reynolds number, $W_s D/\nu$, equal to 2730. To ensure a turbulent flow from the stack, two serrated washers were placed inside the stack at distances of 10 and 12 stack diameters from the orifice.

Concentration profiles were obtained by collecting and passing appropriate air-methane samples through a Beckman Model 400 Hydrocarbon Analyzer, which is a flame ionization detector. Its response time of 0.5 sec was too long to examine any dispersion microstructure. However, time averages can be related to steady-state averages occurring in similar full scale situations. A 2.5-minute averaging time was found to yield stable values of concentration. The sampling rate of the 0.16-cm OD probe was 200 cubic centimeters per minute. The diameter of the sample stream tube thus lies between 1 and 2 millimeters (mm), which represents the spatial resolution. For ground level concentration measurements, the probe was kept slightly above the surface (5 millimeters) to avoid any unnatural surface effects.

Also in Phase II, concentration measurements were made to verify the visualization results of Phase I. The sampling probe was fixed to the wind tunnel surface at a point three ridge heights downstream from the ridge center (base). Pollutants emitted anywhere within the cavity region produced measurable concentrations at the ridge base as a result of intense mixing and recirculation. The reason for locating the sampler near the mountain ridge base was to be certain that measured concentrations could be associated only with recirculation within the cavity. At several downwind locations, the stack was fixed and extended vertically to the height at which no measureable concentrations could be detected at the sampling point. The size of the cavity region determined in this way was found to be in good agreement (Section 6.3) with the results of the smoke visualization portion of the study (Phase I).

The objective of Phase III was to determine the effects that different approach flows might have upon the size and shape of both the smoke envelope and the cavity. Five different cases were examined (Figure 6). The 15-cm Gaussian ridge was used in four cases and a 15° leeward sloping plane was used in a fifth case. Because the ridge height was one-half that of the previously tested ridges, the free-stream velocity for this part of the study was doubled to 6.1 m/sec in order to maintain the same model Reynolds number.

The main reason for the use of a smaller mountain ridge was to more easily accomodate a raised plain stretching from the apex of the ridge upstream to the test section entrance. With the raised plane in place, the smoke envelope and cavity were measured for both a 15-cm natural boundary layer resulting solely from flow over the smooth surface of the wind tunnel (Case A) and for the 60-cm simulated boundary layer (Case B). Measurements were also made for the 60-cm simulated boundary layer flow over a 15° sloping plane placed downstream from the ridge apex (Case C).

For the remaining cases, the upstream plane was removed. The smoke envelope and cavity were measured for both the 15-cm natural boundary layer (Case D) and the 60-cm simulated boundary layer (Case E). Situations characteristic of real atmospheric flow over mountain ridges will most likely have approach flows that lie somewhere between a thick turbulent boundary layer approaching over a raised plane and a thin boundary layer approaching over smooth terrain. The resulting smoke visualized cavity and envelope size measurements are presented and their significance is discussed in Section 6.4.

The wind tunnel ceiling height was adjusted to compensate for blockage effects of the models and to obtain a nonaccelerating free-stream flow above the mountain ridge. The blockage effects of the 30-cm models were more difficult to minimize than those of the 15-cm model. For the 30-cm ridges, the ceiling adjustments that were made resulted in velocity deviations of less than 5 percent. For the 15-cm ridge, deviations were within 2 percent. A 0.65-cm pitot-static probe was used to make longitudinal velocity measurements along the centerline of the wind tunnel. The vertical placement of the probe was well within the free-stream flow away from the floor and ceiling boundary layers.

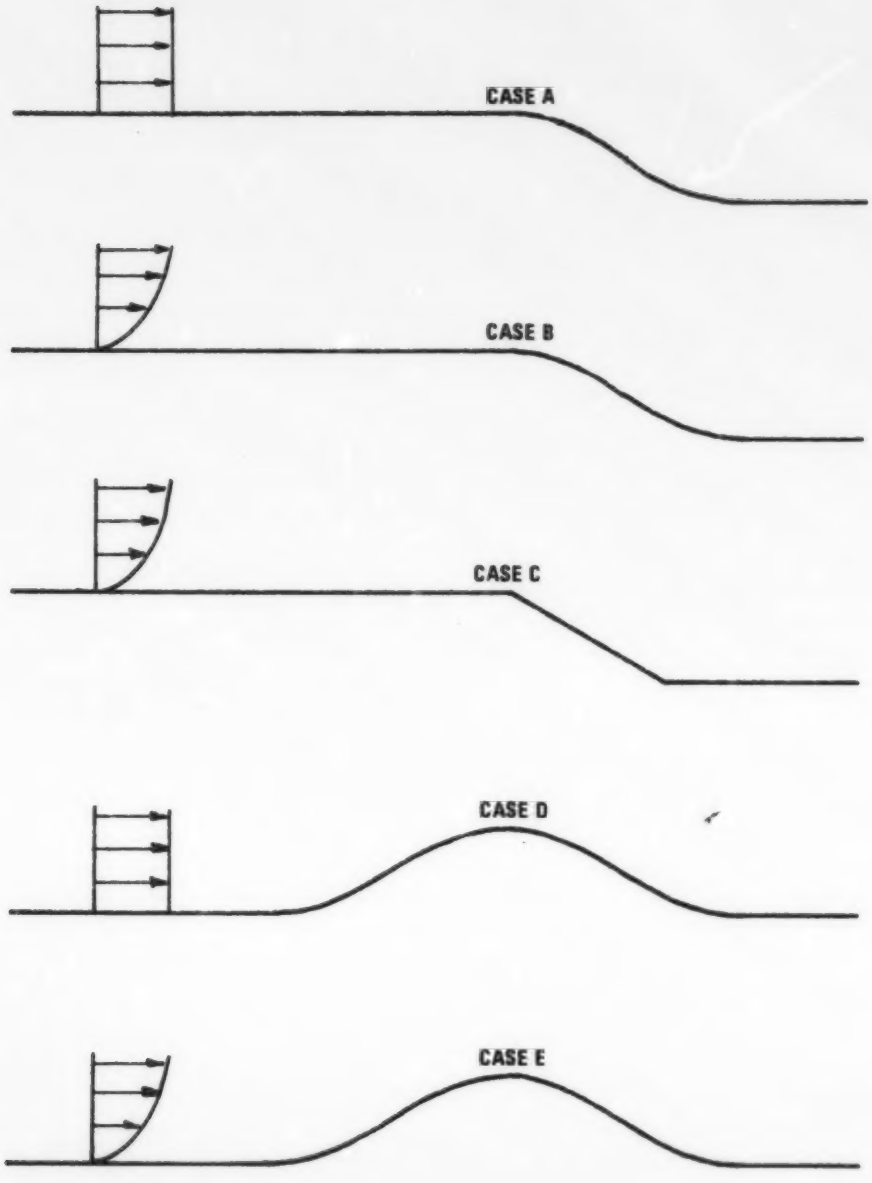

Figure 6. Phase III ridge configurations.

SECTION 6

RESULTS

This section presents those experimental results relevant to describing the flow structure leeward of a mountain ridge. The cavity and envelope sizes and shapes and the mean velocity and turbulence intensity profiles for the Gaussian and triangular ridges at two different flow speeds are compared in Sections 6.1 and 6.2. Section 6.3 presents the concentration data resulting from stacks emitting into the cavity of the Gaussian ridge. The effect of changing the approach flow conditions on cavity and envelope size is presented in Section 6.4.

6.1 PHASE I: ENVELOPE AND CAVITY VISUALIZATION RESULTS FOR 30-cm GAUSSIAN RIDGE AND 30-cm TRIANGULAR RIDGE

In order to have flow separation occurring at the apex of the 30-cm Gaussian ridge, a trip as discussed in the previous section was required. Figures 7 and 8 present the envelope and cavity smoke visualization measurements that were made to demonstrate the effect of forcing separation of the flow at the apex of the ridge and the effect of change in free-stream mean velocity. With flow separation at the apex, the cavity depth and length were two times larger than for the similar cases without the trip, and were independent of the mean flow speed. The change in the free-stream mean velocity showed little visible effects. The flow visualization measurements behind the 30-cm triangular ridge (Figures 9 and 10) result in similar size and shape of both the cavity and envelope as those for the tripped 30-cm Gaussian ridge. The differences in boundary shape near the leeward side of the comparative cavity regions are primarily caused by the increased difficulty in acquiring the visualization measurements. At that position, downwash was less distinct and the smoke was more diffuse, making visualization more difficult. The photographs of Figure 11 show the same envelope shape for the two ridges.

The envelope height measurements in these and other situations to be presented later were only taken to a limited extent downwind. The envelope will continue to grow with increasing distance downwind: however, the magnitude of the flow disturbances associated with the envelope region naturally decreases.

6.2 PHASE I: MEAN VELOCITY AND TURBULENCE INTENSITY MEASUREMENTS FOR 30-cm GAUSSIAN RIDGE AND 30-cm TRIANGULAR RIDGE

The mean velocity and turbulence intensity profiles are presented in Figures 12 through 17 for both upstream and downstream positions from the 30-cm Gaussian ridge and the 30-cm triangular ridge. An identical approach

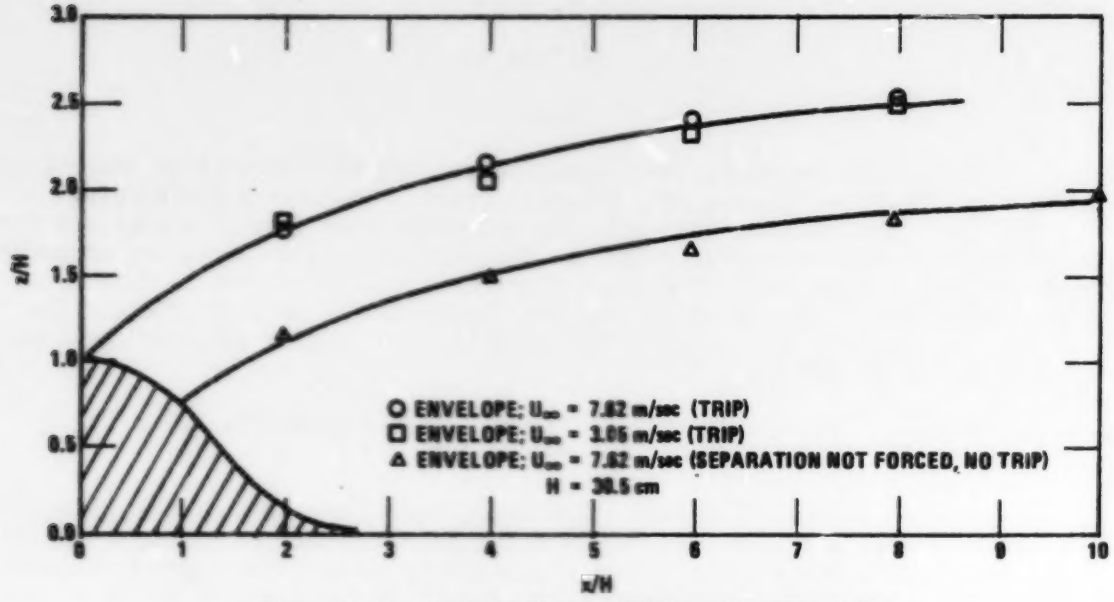

Figure 7. Envelope size in lee of 30.5-cm Gaussian ridge.

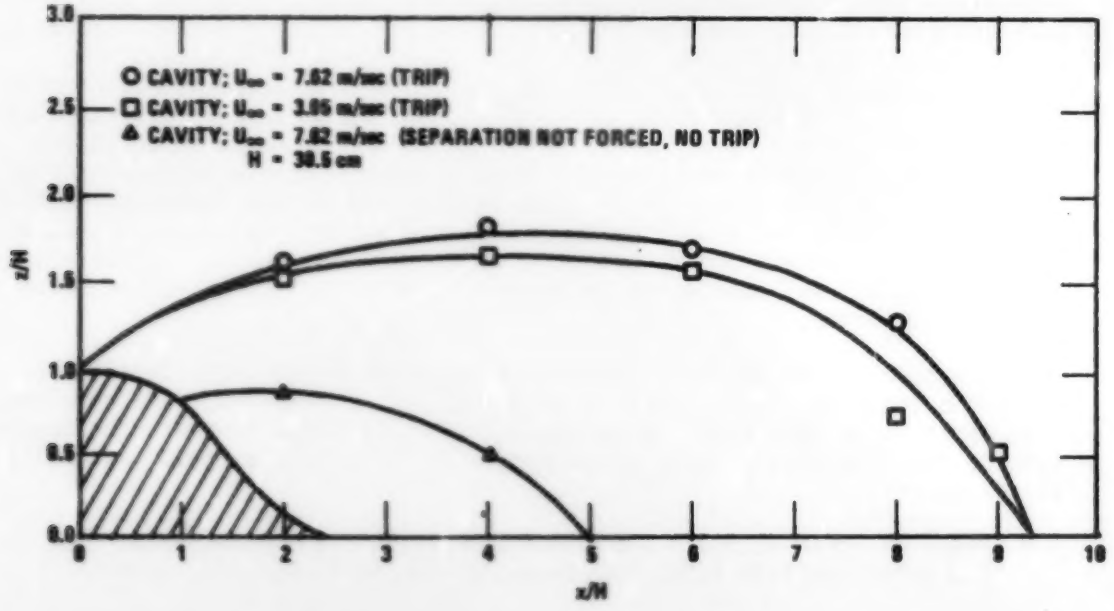

Figure 8. Cavity size in lee of 30.5-cm Gaussian ridge.

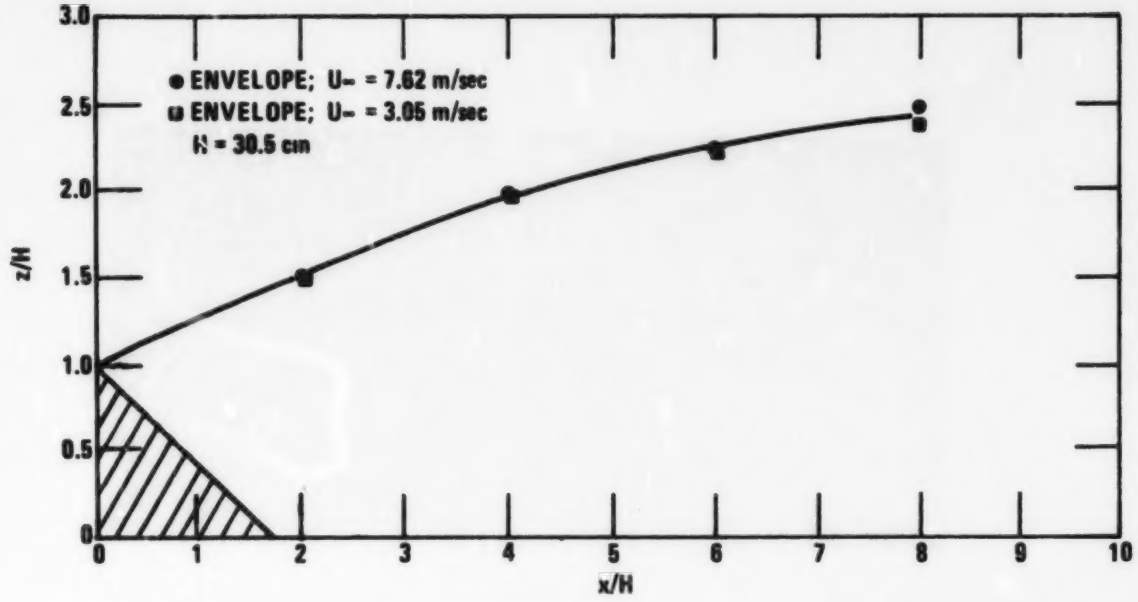

Figure 9. Envelope size in lee of 30.5-cm triangular ridge.

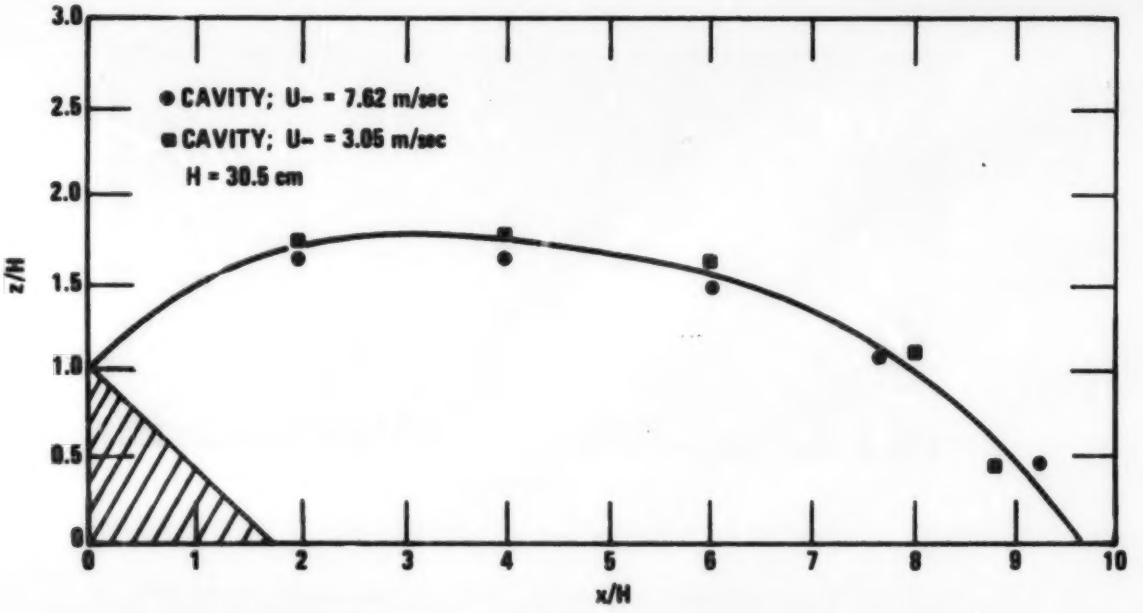

Figure 10. Cavity size in lee of 30.5-cm triangular ridge.

Reproduced from
best available copy.

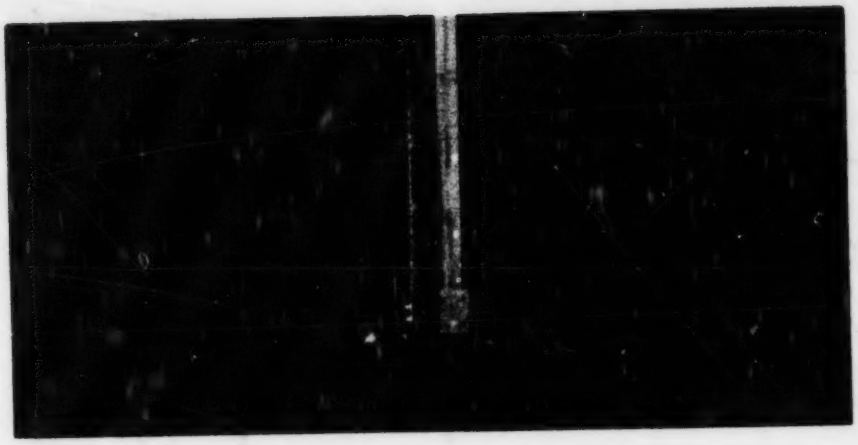

A

B

Figure 11. Smoke envelope in lee of (A) 30-cm Gaussian ridge and (B) 30-cm triangular ridge. (The strut supporting the smoke tube is laterally displaced from the smoke-filled region.)

flow, that is, the 60-cm simulated boundary layer, was used in all cases. The mean velocity, U, is defined as the 1-minute average flow speed in the longitudinal direction, x, at a given position--x, y, z. The turbulence intensity is defined as the standard deviation of the velocity fluctuation in the longitudinal direction, normalized with the mean velocity at the same position. Measurements in regions having mean flow reversals are not quantitatively valid because the hot film cannot distinguish flow direction. Smoke visualization quite clearly revealed upstream flow near the ground level. The data presented, however, should permit valid qualitative comparisons.

The degree of disruption of the approach flow is small in extent, for the untripped ridge (Figures 12 and 13). The trip, however, has a major influence on the flow structure (compare Figures 12 and 13 with Figures 14 and 15). The profiles around the 30-cm triangular ridge (Figures 16 and 17) compare quite well with those of the tripped 30-cm Gaussian ridge (Figures 14 and 15). Note that, for all cases, the profiles are independent of the free-stream mean velocity. The mean velocity profiles at the upstream base location for all cases are similar to a one-third power law profile. The change from the one-seventh power law profile of the approach flow (Figure 4) is caused by upstream blocking induced by the model ridge.

Included in Figure 14 are data obtained far downstream from the cavity region. Note the three distinct parts of the mean velocity profile. The bottom part represents the newly developing boundary layer, which has a one-seventh power law profile, as expected. The middle part represents the region of the readjusting boundary layer; the top part represents that of the undisturbed boundary layer.

6.3 PHASE II: CONCENTRATION MEASUREMENTS FOR STACK PLACED IN LEE OF 30-cm GAUSSIAN RIDGE

Concentration measurements are presented in order to assist in describing plume behavior within the cavity region. To present the data in a form for easy comparison, the measured concentrations have been nondimensionalized with the stack gas concentration, C_s. Thus, in the figures, the value C, percent, is the measured concentration expressed as the percentage of stack gas concentration. These data can be related to field situations as discussed in Section 4.

The concentration values in Figure 18 were detected by a ground level probe located near the base of the 30-cm Gaussian ridge. The stack was positioned at four different downwind locations and raised in increments in the vertical while the probe sampled at a fixed position. The vertical position at which no ground concentrations were detected defined the upper limit of the cavity. The cavity size thus determined is similar to that found from smoke visualization (Section 6.1). Also note the similarity in the concentration plots and the fact that significant ground level concentrations are found upwind of the stack.

Figure 19 gives the resulting ground level concentrations downwind from a stack placed at the leeward ridge base for three stack heights. The

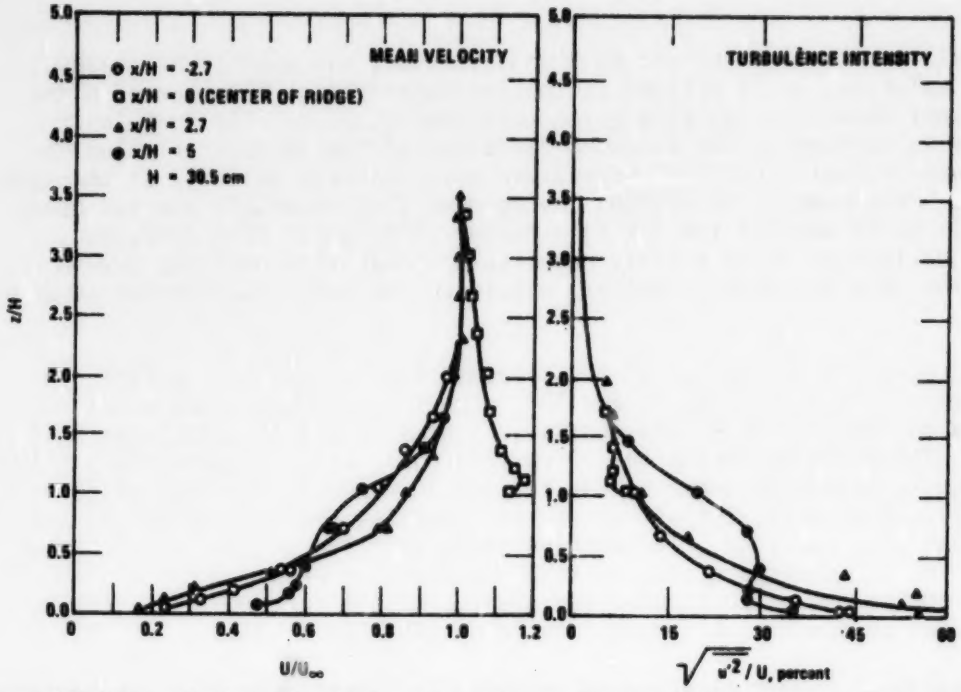

Figure 12. Mean velocity and turbulence intensity profiles for 30.5-cm Gaussian ridge (separation not forced), U_∞ = 3.05 m/sec.

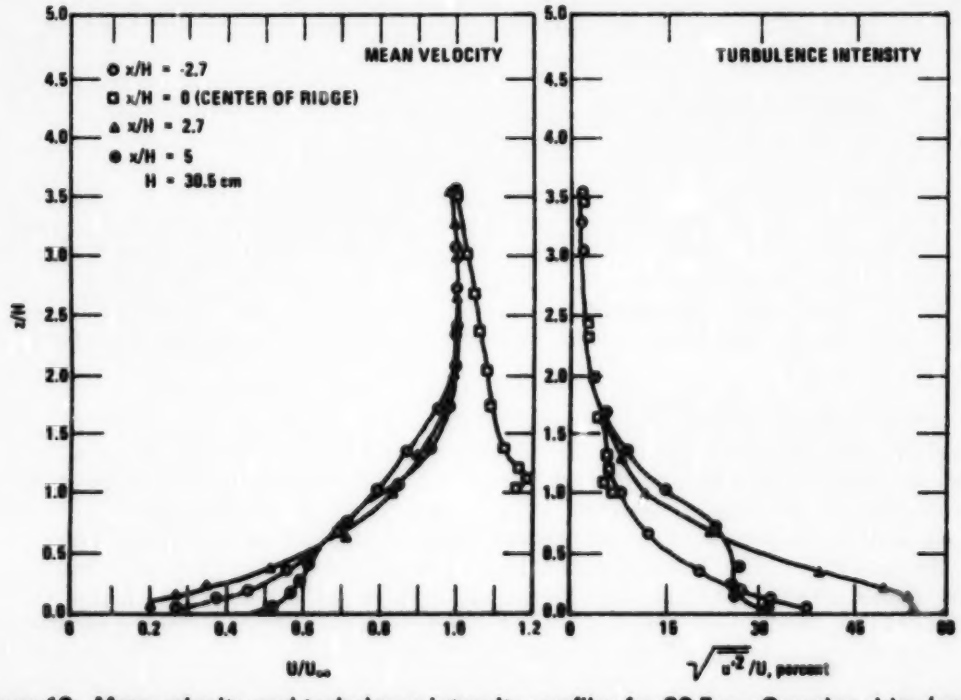

Figure 13. Mean velocity and turbulence intensity profiles for 30.5-cm Gaussian ridge (separation not forced), U_∞ = 9.15 m/sec.

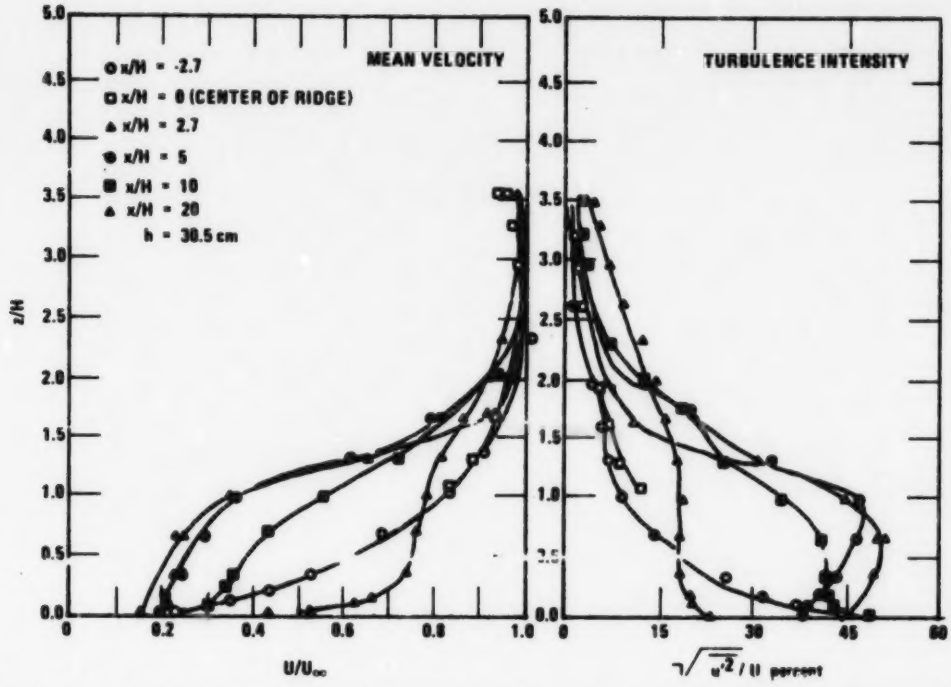

Figure 14. Mean velocity and turbulence intensity profiles for the 30.5-cm Gaussian ridge, U_∞ = 3.05 m/sec.

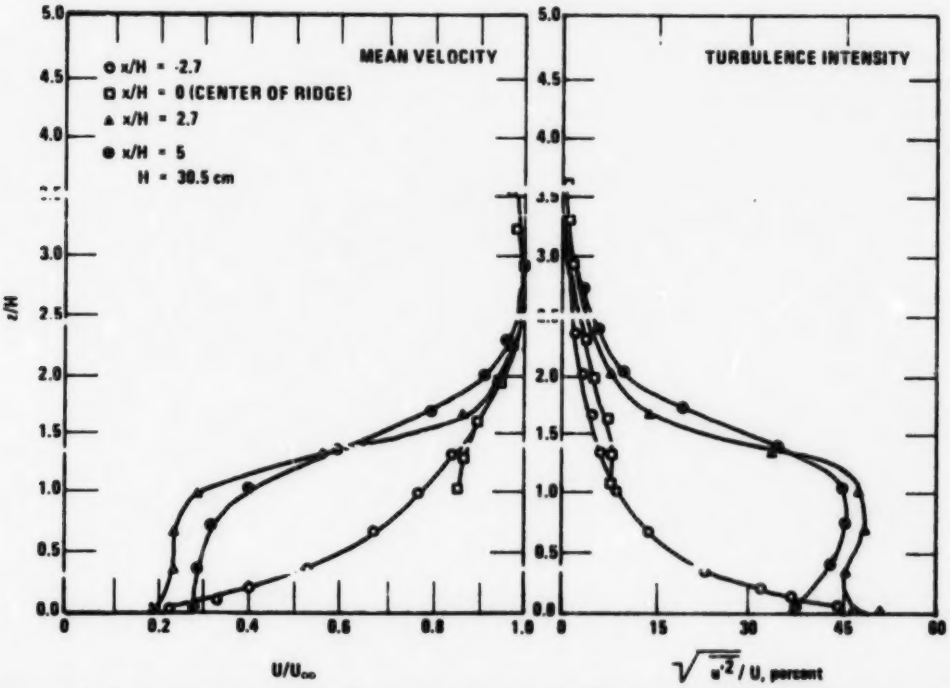

Figure 15. Mean velocity and turbulence intensity profiles for the 30.5-cm Gaussian ridge, U_∞ = 9.15 m/sec.

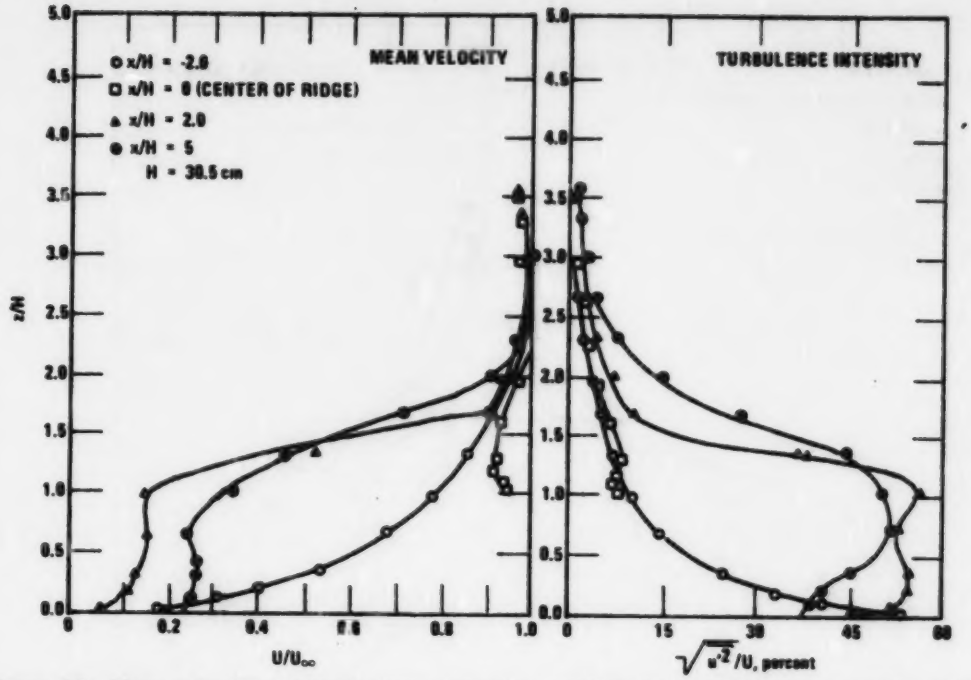

Figure 16. Mean velocity and turbulence intensity profiles for the 30.5-cm triangular ridge, U_∞ = 3.05 m/sec.

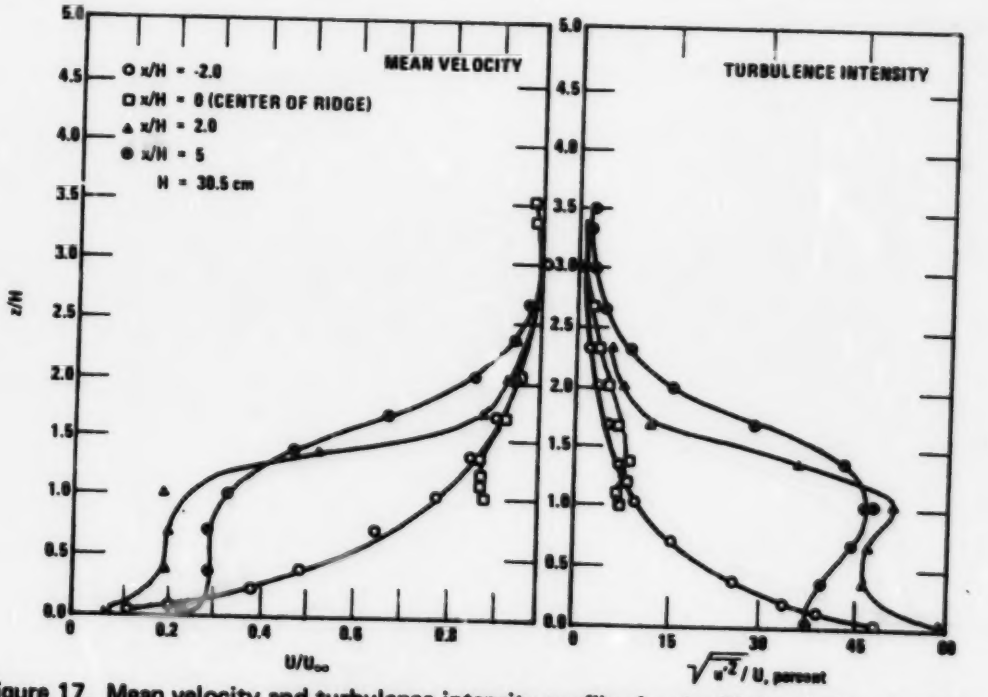

Figure 17. Mean velocity and turbulence intensity profiles for the 30.5-cm triangular ridge, U_∞ = 9.15 m/sec.

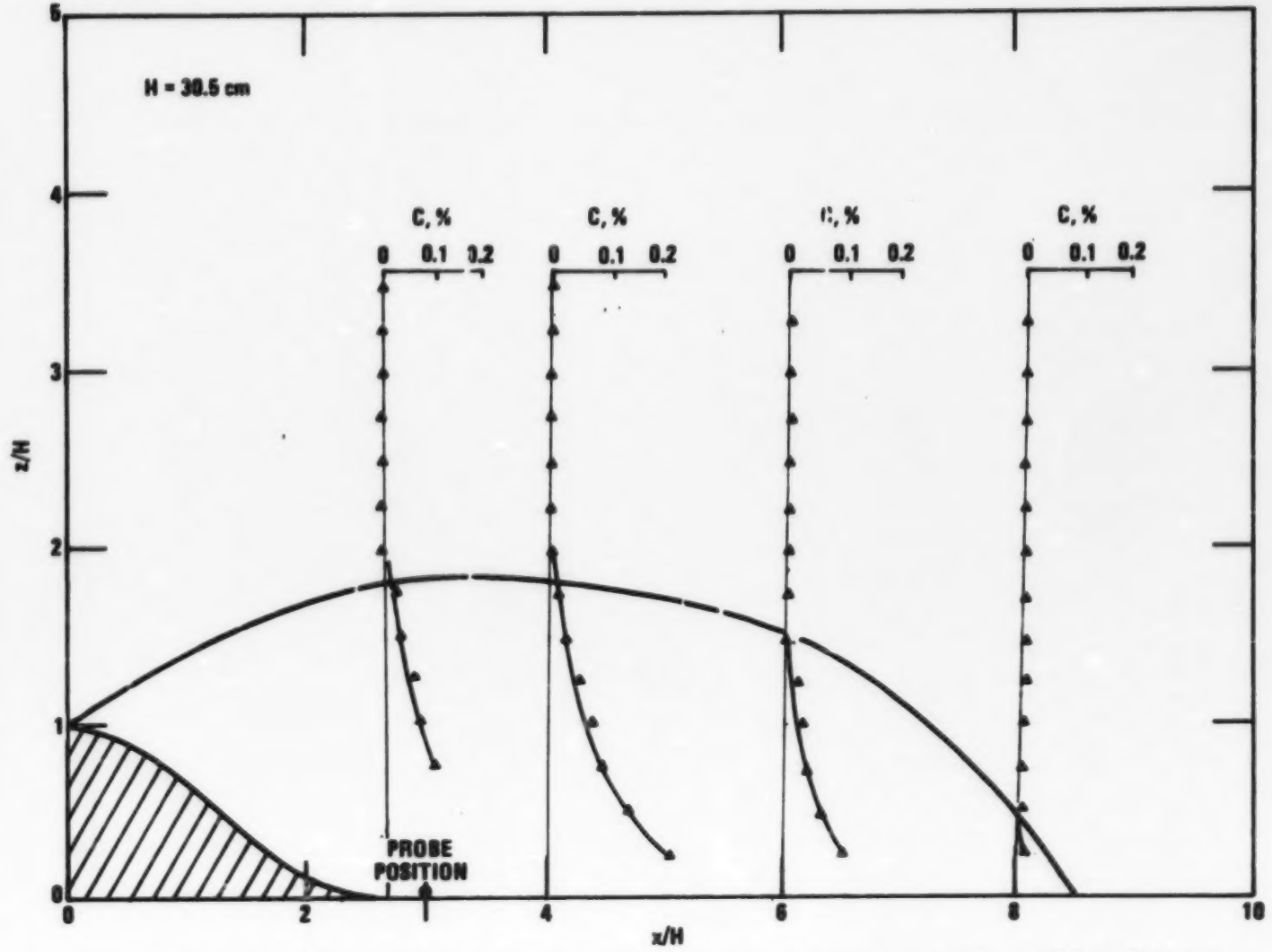

Figure 18. Ground level concentrations measurements with sampling probe fixed near base (x/H = 3 from ridge center, z/H = O) of 30.5 cm Gaussian ridge. (Stack was placed at four downwind locations and its height was varied).

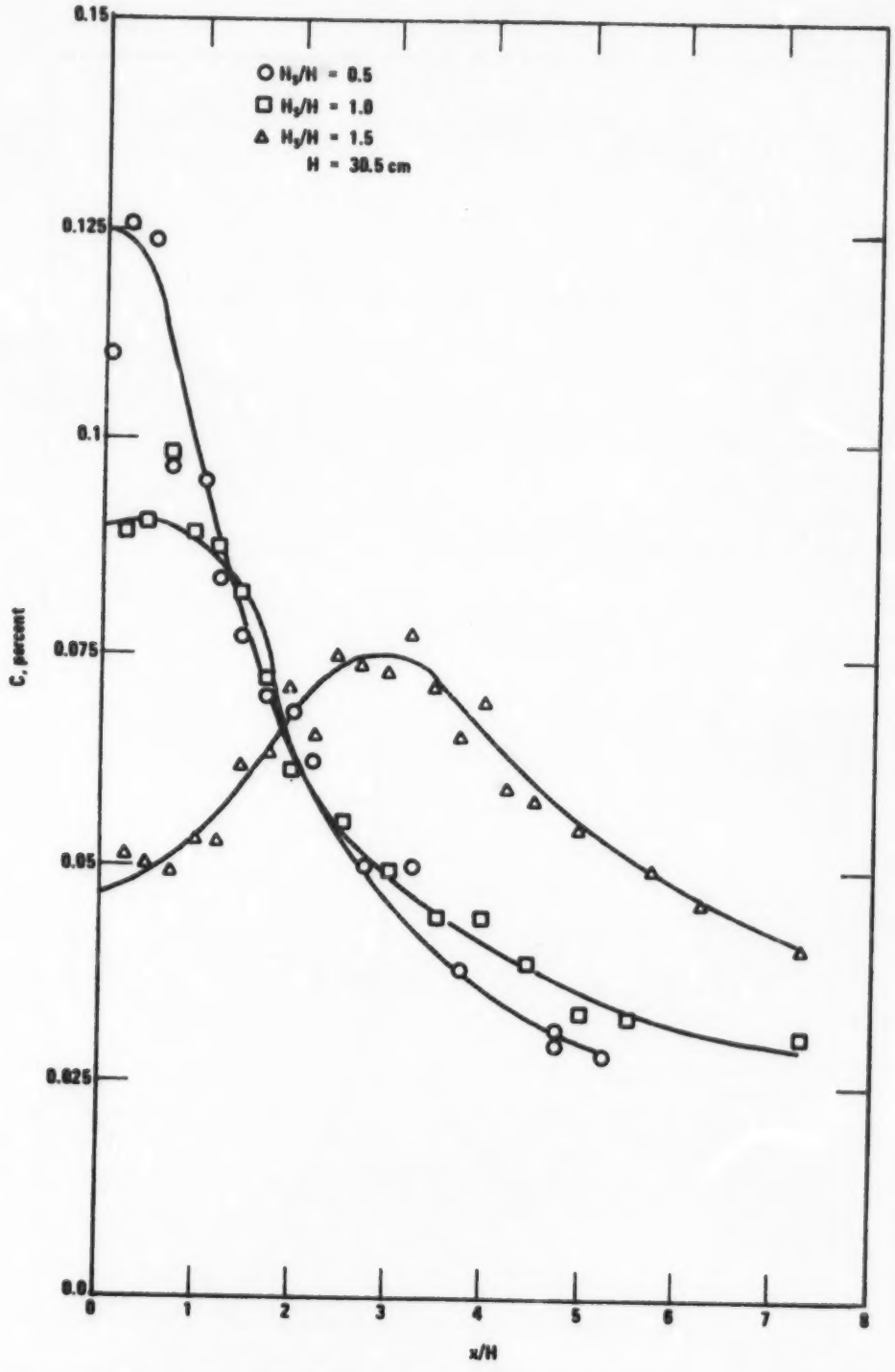

Figure 19. Longitudinal ground level concentration profiles downwind from stack placed at base (x/H = 2.7 from center) of 30.5-cm Gaussian ridge.

points of maximum concentration are found very close to the stack base, perhaps even upwind of the stack base. The peak concentration decreases and is shifted downwind as the stack height increases. This is typically found to occur over smooth terrain. Beyond two ridge heights downwind from the stack, however, the concentrations are highest for the elevated stack.

Figure 20 presents the vertical concentration profiles in the lee of the 30-cm Gaussian ridge. The stack was fixed at the ridge base with H_s/H equal to 0.5. Because of the nearly stagnant mean flow in the lee of the ridge and the general upward flow in the cavity region along the ridge surface, a substantial plume rise occurs as indicated by the vertical concentration profile. The concentrations on the leeward side of the cavity are more uniform than those farther upstream, but little spreading occurs into the region above the cavity ($z/H = 2$, as determined in Figure 18). The photographs of Figure 21 show two realizations of the plume from the short stack. These photographs show the substantial plume rise and very wide dispersion in both the upwind and downwind directions and the large unsteadiness of the flow. The lateral concentration profiles (Figure 22 through 24) show that the lateral plume width changes only slightly in the downwind direction. Figure 25 vividly demonstrated how rapidly the pollutants are diluted along the downwind direction near the elevation of the maximum concentration.

Additional concentration measurements for the same stack, elevated to a height 1.5 times the ridge height, were also made. Figure 26 presents a few vertical concentration profiles for the elevated stack and shows the plume rise to be essentially zero. Zero plume rise occurs because the elevated stack while in the cavity is above the region of mean flow stagnation. The elevation of the point of maximum concentration decreases with downwind distance, showing evidence of the recirculation within the cavity. The highly uniform concentrations below $z/H = 1$ are also evidence of the recirculation. The photographs of Figure 27 show three realizations of the plume from the tall stack. The small plume rise, the large unsteadiness of the flow, and the wide vertical dispersion are evident. Even for this elevated stack, however, little dispersion into the region above the cavity occurs. The lateral ground level concentration profiles (Figure 28 and 29) show essentially identical spreads with only minor differences in their values near the center ($y/H = 0$). From these results, it is evident that instead of the strong immediate downwash that occurred for the shorter stack, the taller stack emissions are caught in the outer recirculation region within the cavity. The direction of the recirculation is down the leeward side of the cavity and upstream along the ground.

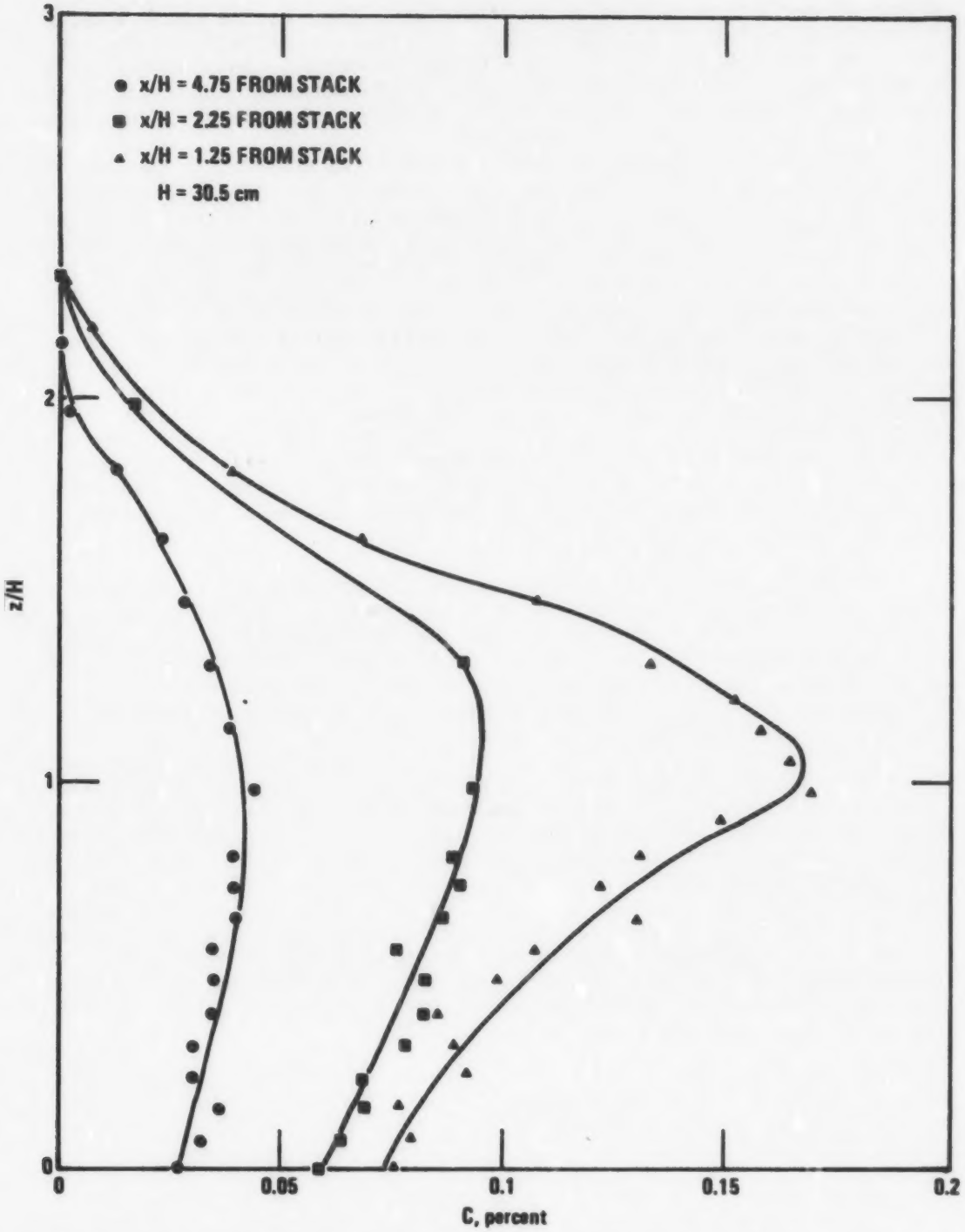

Figure 20. Vertical concentration profiles for stack placed at base (x/H = 2.7 from center) of 30.5 cm Gaussian ridge, $H_s/H = 0.5$.

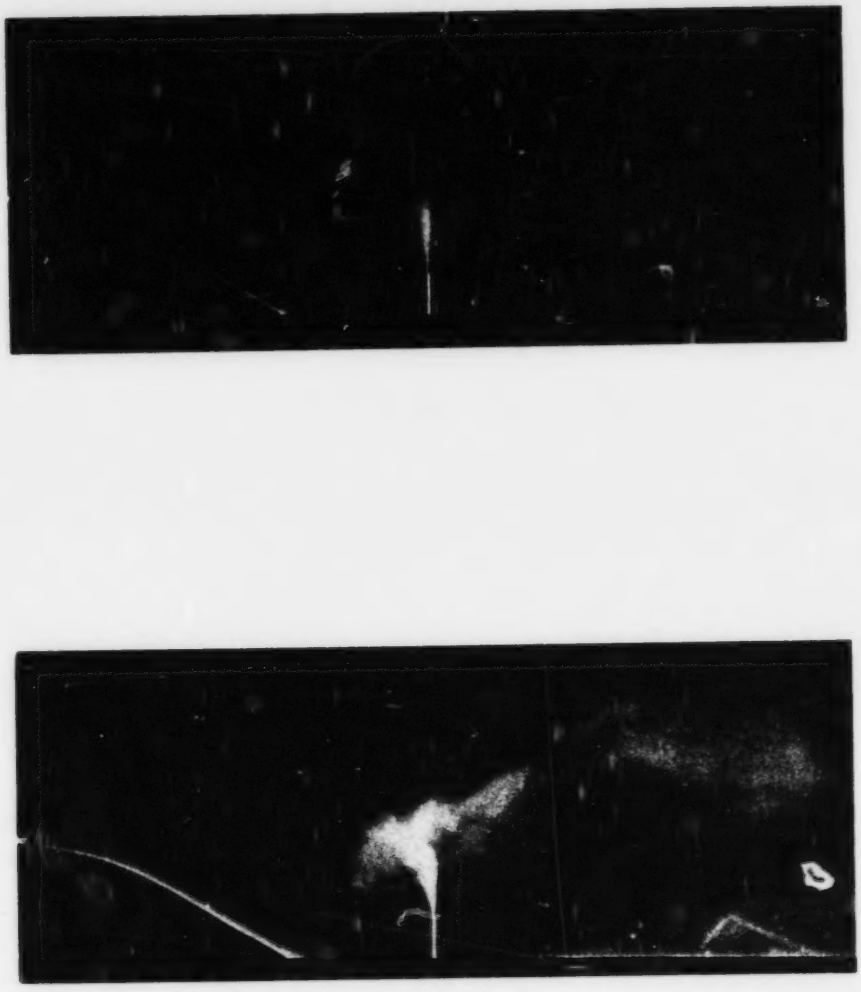

Figure 21. Smoke visualization with 0.5-H stack placed at base of 30-cm Gaussian ridge (x/H = 2.7 from ridge center).

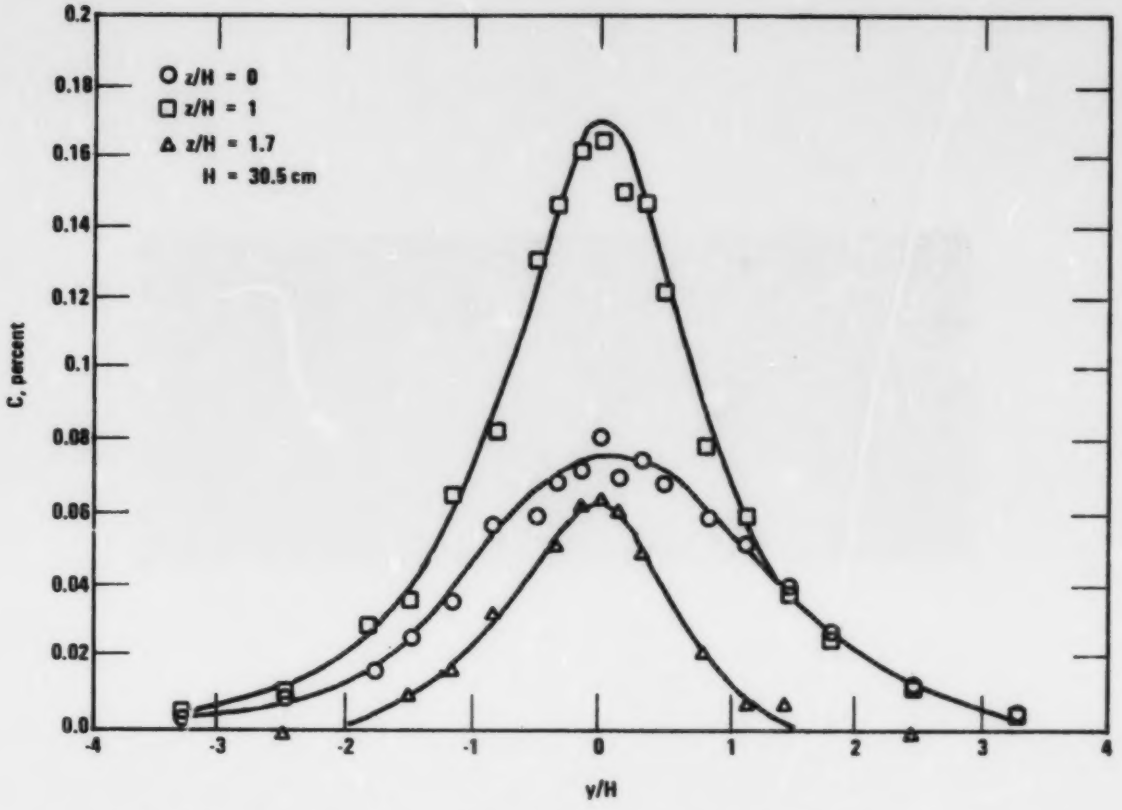

Figure 22. Lateral concentration profiles from stack placed at base (x/H = 2.7 from center) of 30.5-cm Gaussian ridge, x/H = 1.25, $H_s/H = 0.5$.

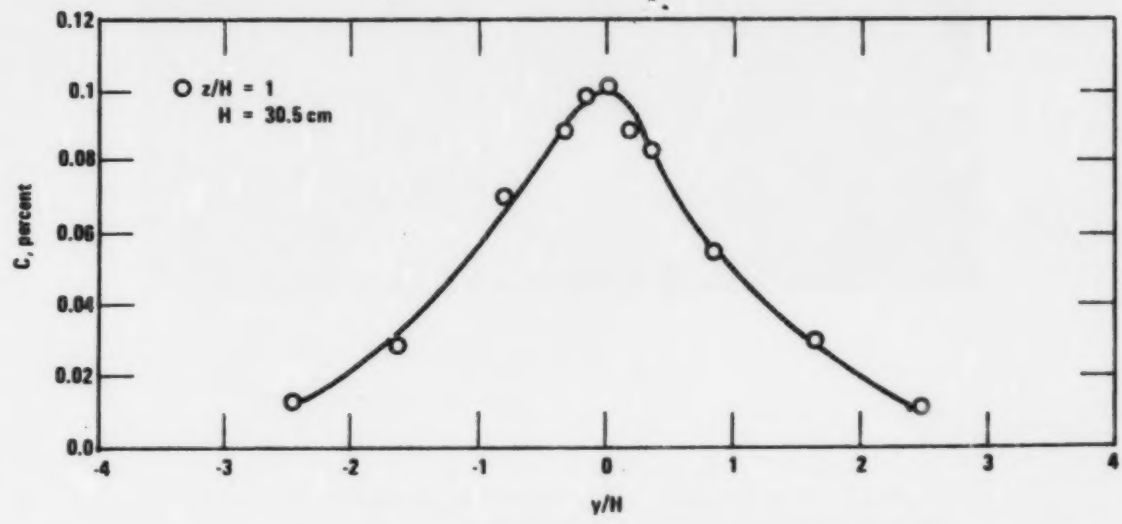

Figure 23. Lateral concentration profile from stack placed at base (x/H = 2.7 from center) of 30.5-cm Gaussian ridge, x/H = 2.25, $H_s/H = 0.5$.

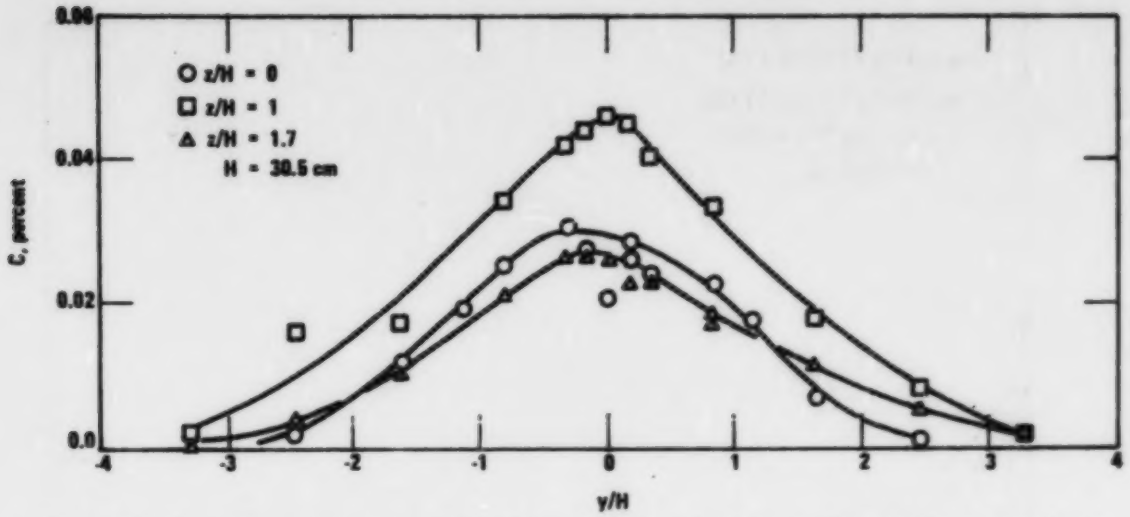

Figure 24. Lateral concentration profiles from stack placed at base (x/H = 2.7 from center) of 30.5-cm Gaussian ridge, x/H = 4.75, H_s/H = 0.5.

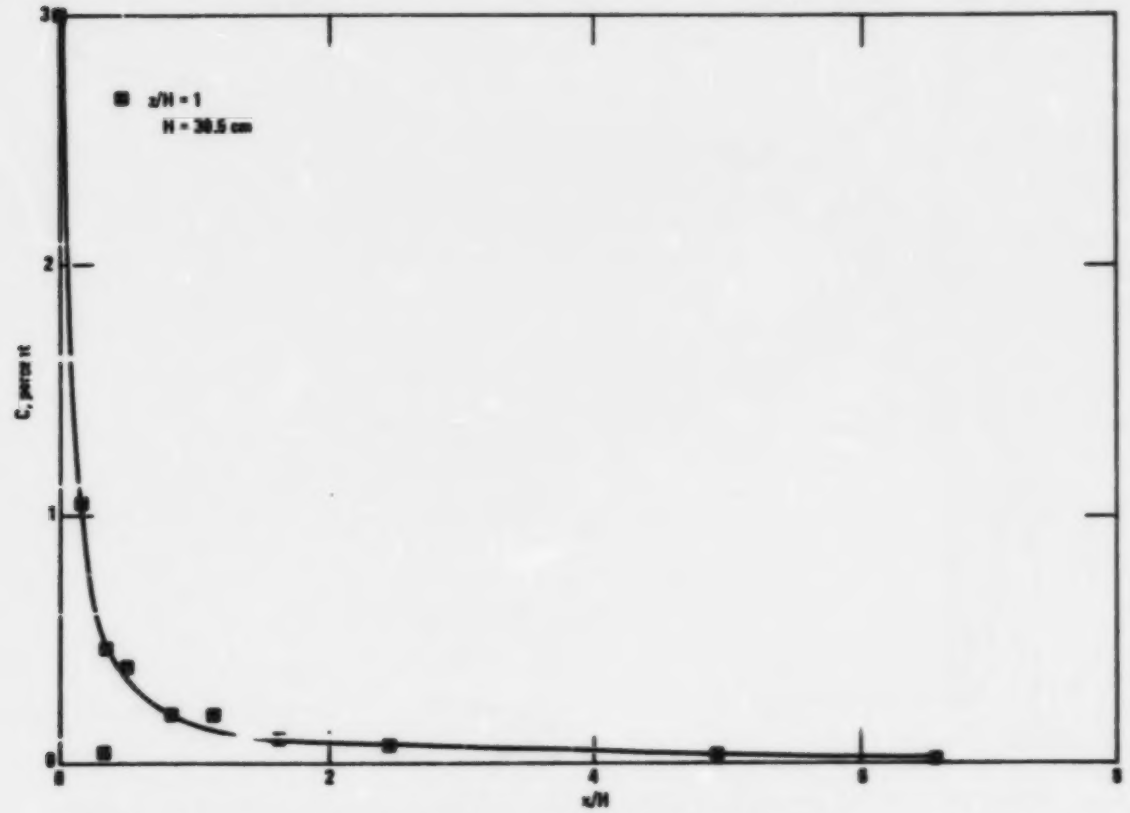

Figure 25. Elevated longitudinal concentration profile downwind from stack placed at base (x/H = 2.7 from center) of 30.5-cm Gaussian ridge, H_s/H = 0.5.

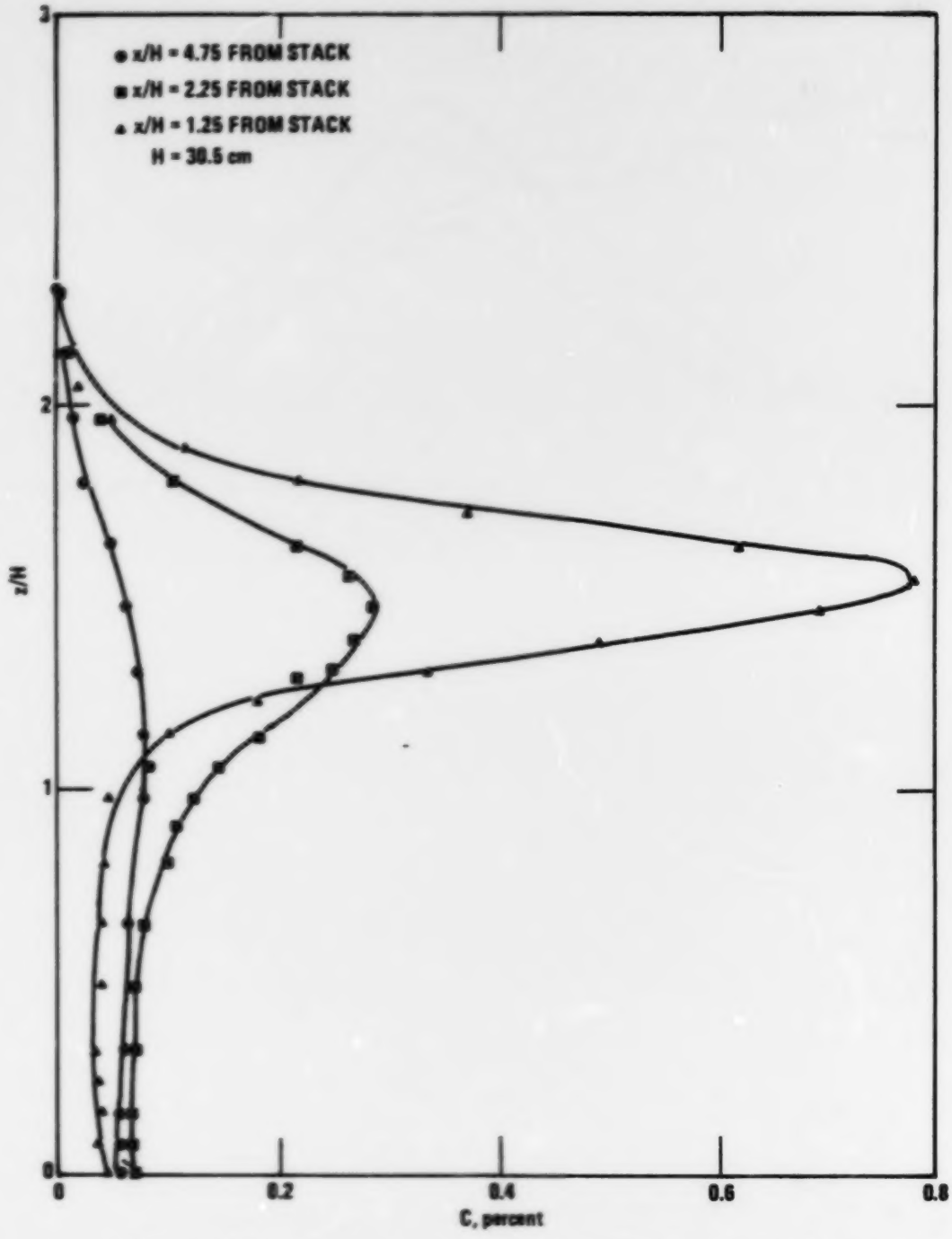

Figure 26. Vertical concentration profiles for stack placed at base (x/H = 2.7 from center) of 30.5 cm Gaussian ridge, $H_s/H = 1.5$.

Reproduced from
best available copy.

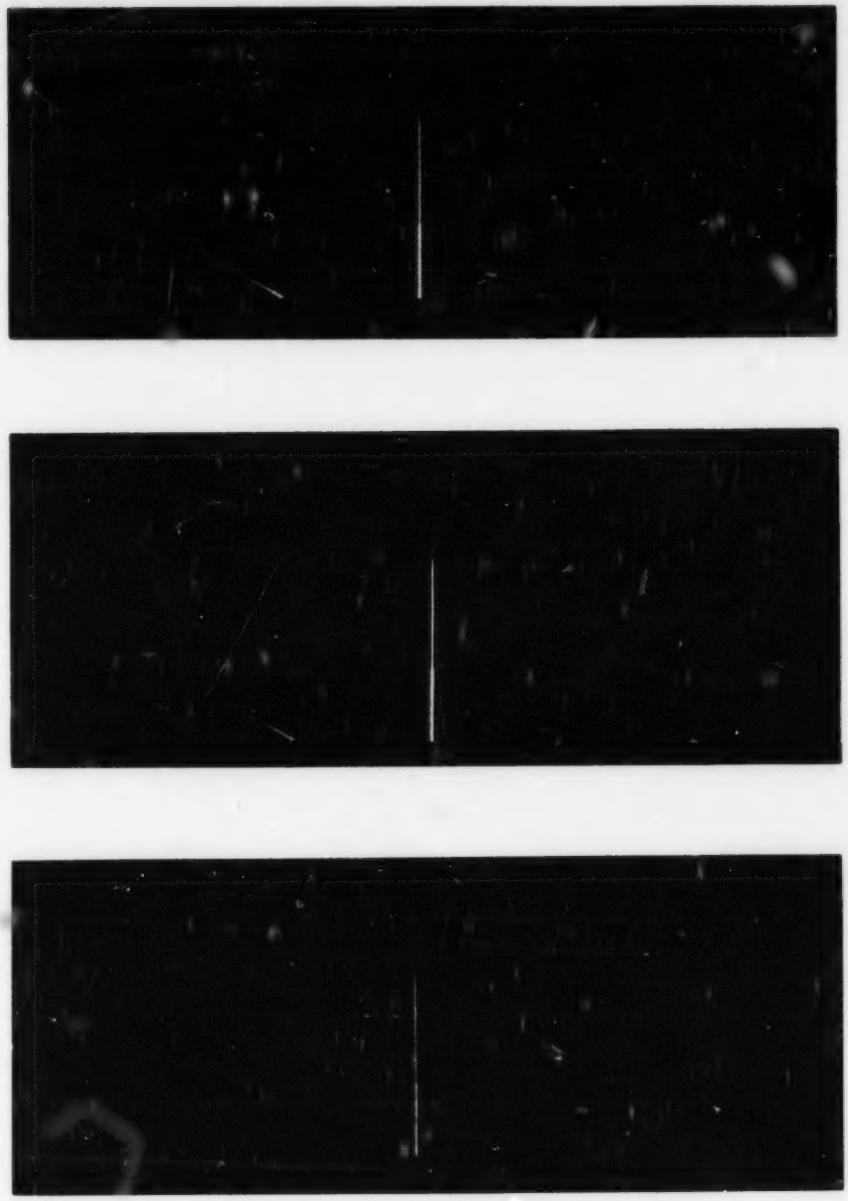

Figure 27. Smoke visualization with 1.5 H stack placed at base of 30-cm Gaussian ridge (x/H = 2.7 from ridge center).

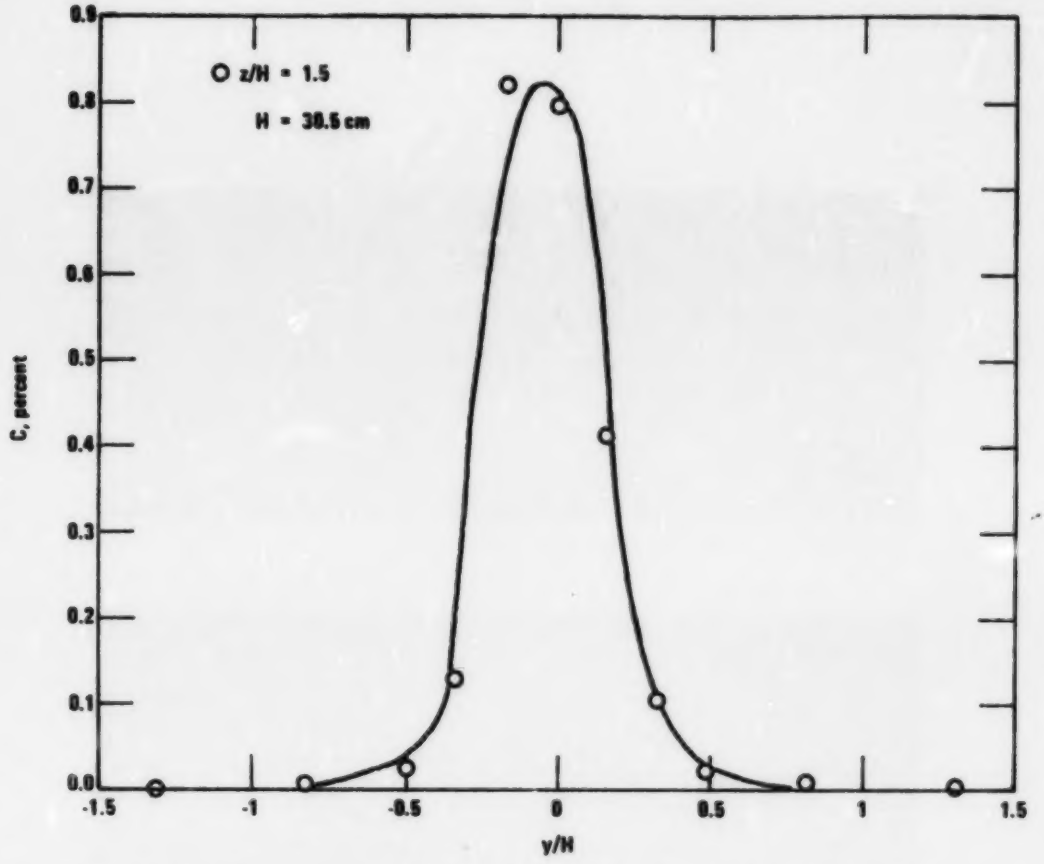

Figure 28. Lateral concentration profile from stack placed at base (x/H = 2.7 from center) of 30.5-cm Gaussian ridge, x/H = 1.25, H_s/H = 1.5.

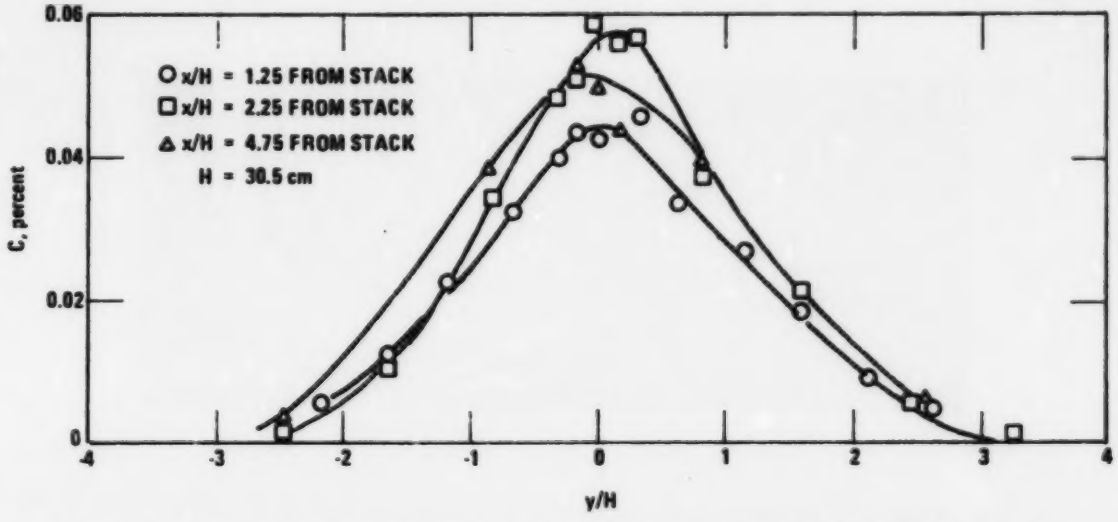

Figure 29. Lateral ground level concentration profiles from stack placed at base (x/H = 2.7 from center) of 30.5-cm Gaussian ridge, z/H = 0, H_s/H = 1.5.

6.4 PHASE III: CAVITY AND ENVELOPE MEASUREMENTS IN LEE OF 15-cm GAUSSIAN RIDGE

The goal was to determine what effect the approach boundary layer conditions have on the size and shape of the leeward cavity region. Figures 30 through 35 contain the results of the third phase of this study. In addition to the cavity and envelope measurements, some mean velocity profiles taken with a pitot-static tube above the ridge center were included.

Figure 30 shows the resulting cavity size and envelope for the 60-cm simulated boundary layer approaching the 15-cm Gaussian ridge (Case E), which is similar to that used in Phase I. The boundary layer thickness to ridge height ratio was four (double that for the 30-cm ridge); however, little difference in the size or shape of the cavity or envelope region resulted (compare with Figure 7 and 8).

With the vortex generators and roughness removed (Case D), the resulting natural boundary layer over the smooth tunnel floor was found to be 15 cm in depth, so that the boundary layer to ridge height ratio was about 1. The mean velocity profile over the ridge center (Figure 31, Case D) was found to jet and also to have a slightly larger shear in comparison with the 60-cm simulated boundary layer flow over the 30-cm Gaussian ridge (Figure 14). The turbulence levels for the natural boundary layer may be expected to be much less than those of the simulated atmospheric boundary layer. These differences could explain the slightly larger extent of the cavity region (compare Figures 30 and 8 to Figure 32). The depth of the envelope agrees well with those of Case E (Figure 30) and the similar case in Phase I (Figure 7).

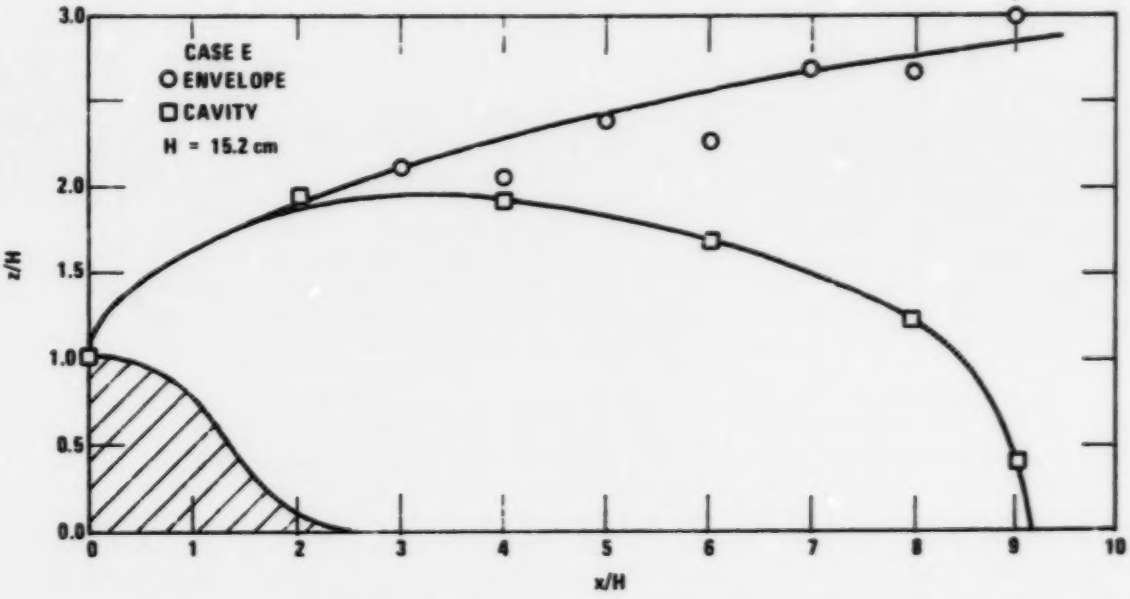

Figure 30. Envelope and cavity size in lee of 15.2-cm Gaussian ridge (60-cm simulated boundary layer).

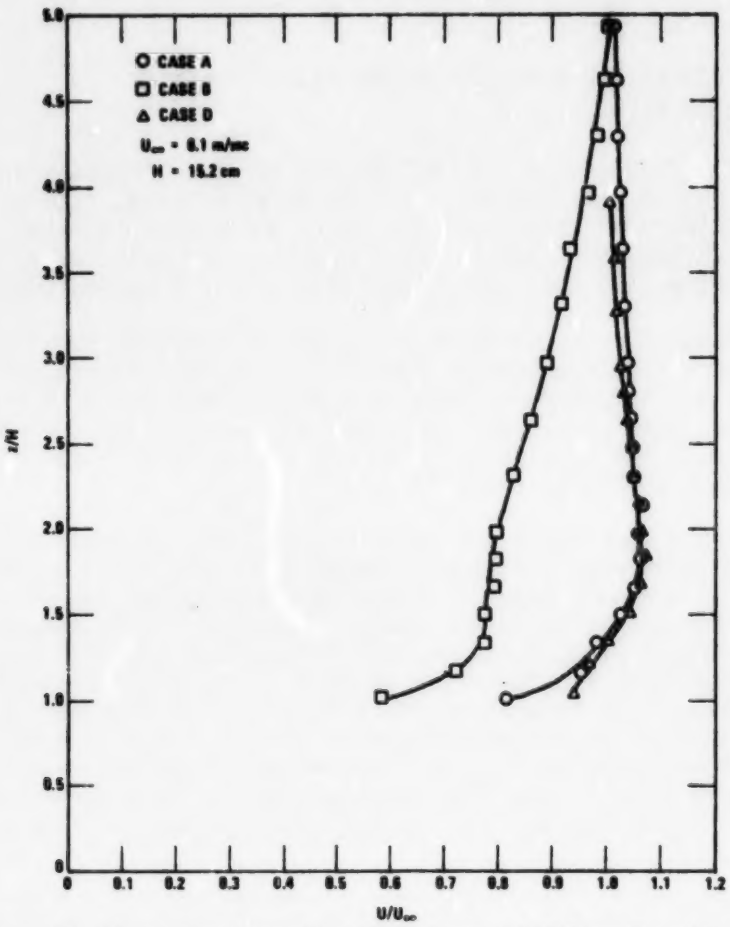

Figure 31. Mean velocity profiles above center of 15.2-cm Gaussian ridge.

Changes in the size of both the cavity and envelope were found when the mean flow approached the ridge along a raised plane elevated to the height of ridge apex. Figure 31 presents the mean velocity profile above the center of the ridge for the 15-cm natural boundary layer (Case A), which is shown to be similar to that of Case D. Both the wake and envelope size (Figure 33), however, are significantly reduced in comparison with the previous cases (D and E) for an isolated ridge. Very similar results were found for the situation with the 60-cm simulated boundary layer (Case B, Figure 34). The effect of changing the boundary layer conditions appears to be minor.

The upwind terrain has been shown to have a direct effect on the size of the cavity and envelope. In addition, angle of downslope from the ridge apex can also have an effect on the size of the cavity region. With small slope angles, the adverse pressure gradient in the lee of the ridge may be expected to be lower, which would result in a smaller stagnation region. The envelope and cavity size in the lee of a 15° slope (Case C) is shown in Figure 35. The approach flow conditions were identical to Case B (Figure 31). As expected, the cavity size is reduced significantly.

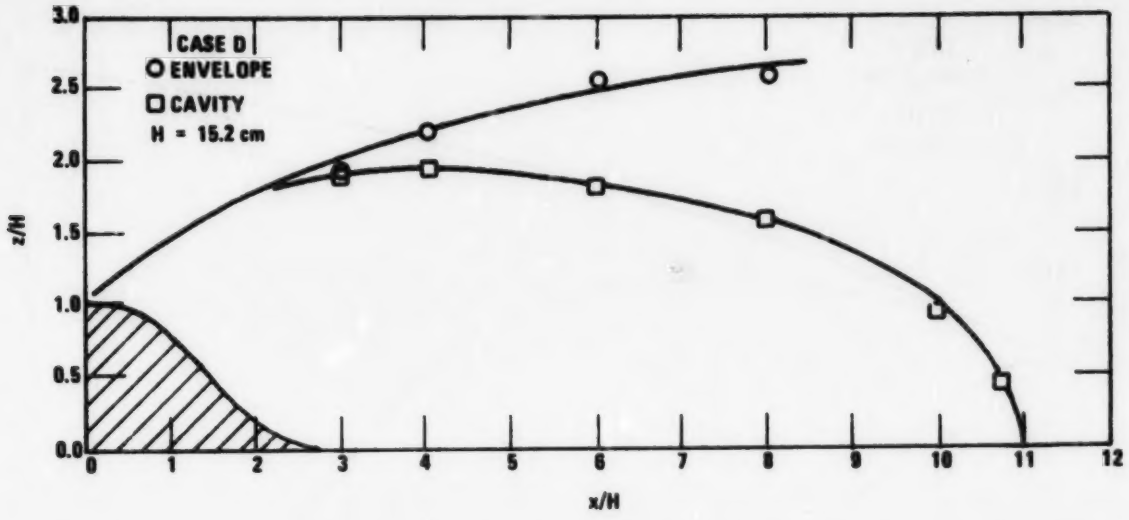

Figure 32. Envelope and cavity size in lee of 15.2-cm Gaussian ridge (15-cm natural boundary layer).

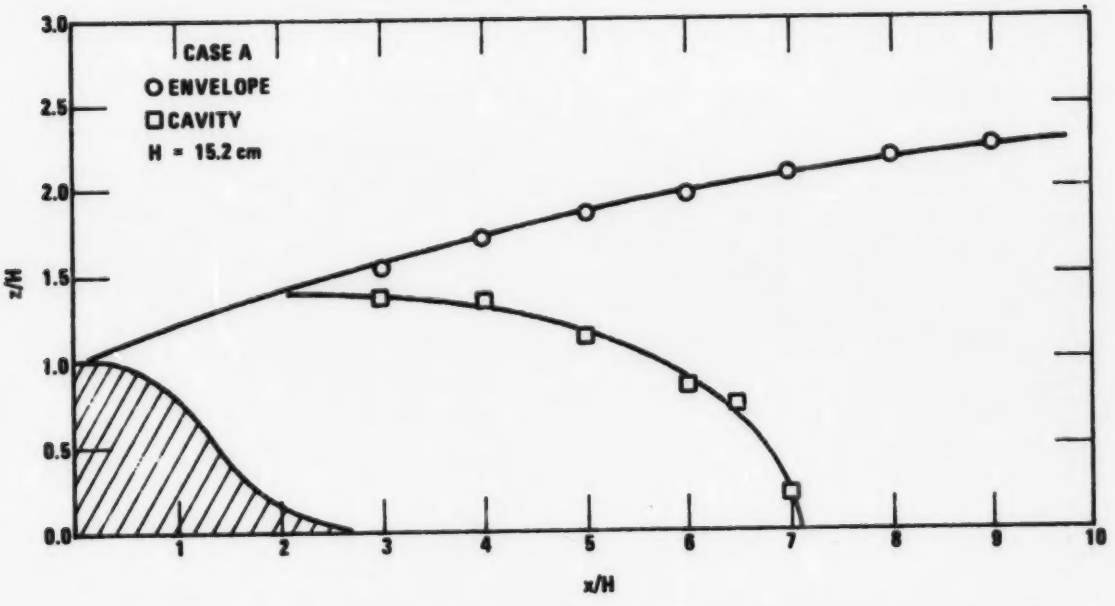

Figure 33. Envelope and cavity size in lee of 15.2-cm Gaussian ridge (15-cm natural boundary layer with raised plane approach).

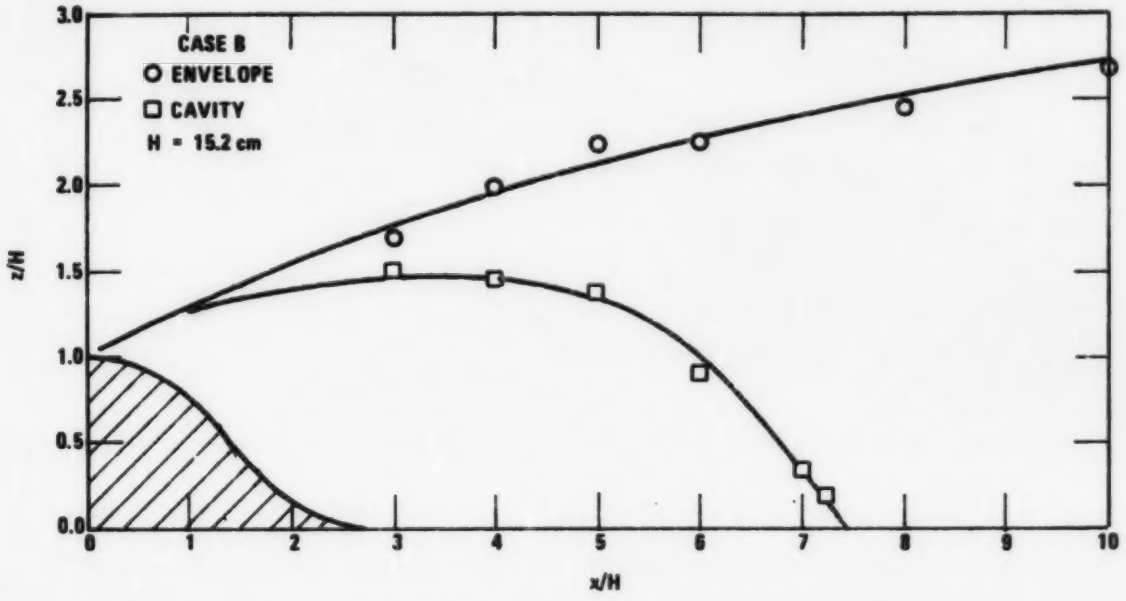

Figure 34. Envelope and cavity size in lee of 15.2-cm Gaussian ridge (60-cm simulated boundary layer with raised plane approach).

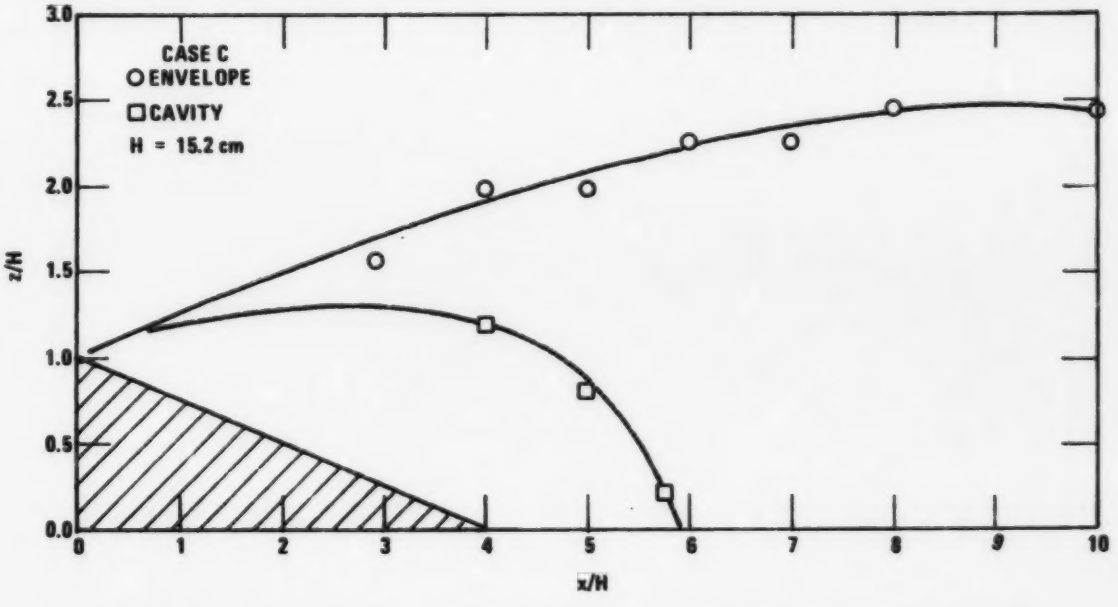

Figure 35. Envelope and cavity size in lee of 15° sloping plane (60-cm simulated boundary layer with raised plane approach).

SECTION 7

DISCUSSION AND SUMMARY

On the lee side of a mountain ridge, under neutral atmospheric conditions, there is a highly turbulent region in which significant plume downwash and mixing occurs. This region, which is caused by the main flow separating from the leeward surface of the ridge, is characterized by a general air recirculation and is referred to as the cavity. Although other types of phenomena are expected to occur in nonneutral flows, a firm understanding of the more simplistic neutral flow is a necessary first step. Neutrally stratified and moderate to high wind conditions offer the greatest potential for the natural occurrence of a separated flow region similar to that examined in this study.

The literature search reported in Section 3 revealed little detailed information that would relate the size or extent of the cavity to either the downslope shape or the mean flow characteristics. The field studies do, however, strongly support the assertion that a recirculating flow region with strong downwash and dispersion characteristics often exists on the leeward side of a ridge. A ridge with a salient peak or a steep sloping side can be expected to exhibit separation at its apex. Under this circumstance, the cavity will be its largest, both in depth and horizontal extent.

For the model Gaussian ridge, the point of separation was found to occur considerably downstream from its apex, and flow visualization showed the point of separation to fluctuate widely in position from one instant of time to the next. In order to demonstrate the maximum possible extent of the cavity, the main flow was forced to separate at its apex. Under neutral stability and high wind speed conditions, the model results can be expected to represent actual results behind similarly shaped ridges that exhibit mean flow separation at their apexes.

For the 30-cm Gaussian ridge with separation occurring at its apex, the maximum depth and horizontal extent of the cavity region were found to be 2 H and 10 H, respectively. Similar results were found for the 30-cm triangular ridge. The mean velocity and turbulence intensity profiles were also found to be similar for the two ridges. Thus, the flow patterns in the lees of ridges that exhibited separation at their apex were found not to be sensitive to the detailed shape of the downslope.

Cavity sizes in the lee of the tripped 15-cm Gaussian ridge were measured with four different approach flows. With the 60-cm simulated boundary layer approach, which was similar to the situation examined for the 30-cm ridge, the maximum depth and horizontal extent were found to be 2 H and 10 H,

respectively. The cavity sizes and shapes were found to be only slightly affected by the thickness and intensity of the approach boundary layer, but to be fairly strongly dependent upon the upwind terrain and the gross features (angle) of the downslope.

An important objective of this study was to demonstrate the behavior of a plume emitted from a stack placed within the cavity region. The 30-cm Gaussian ridge with separation occurring at its apex and a stack emitting an air-methane mixture as a tracer gas were used. The size of the cavity determined from the tracer gas measurements showed a maximum depth and horizontal extent of 2 H and 8.5 H, respectively. The horizontal extent was only slightly smaller than that found by smoke visualization for the same situation.

Ground level concentrations were sampled through a probe fixed near the base of the ridge (3 H) for several stack heights with the stack placed at 2.7 H, 4 H, 6 H, and 8 H downwind. At all stack positions, the measured ground level concentration increased with the lowering of the stack height. The fact that significant ground level concentrations are found at a distance of 5 H upwind of the stack confirms the existence of a strong recirculating flow within the cavity region.

In order to quantitatively demonstrate the types of plume behavior that exist for stack emissions within the cavity, longitudinal, lateral, and vertical concentration profiles were taken throughout the cavity region for three stack heights with the stack fixed at the base of the ridge. A stack placed at this location results in measured concentrations (order of magnitude) that might occur if the stack were placed elsewhere downwind in the cavity. Flow visualization and the concentration measurements aloft support this assertion. For a stack positioned further upwind and along the ridge slope, the upslope flow would dominate. This may provide characteristically different concentration profiles.

With the stack positioned at the downwind base of the ridge, longitudinal ground level concentration profiles were measured for three stack heights. For the 0.5 H and the 1 H stack, the highest concentrations were found at a position very near the stack. This is an indication of strong immediate downwash. For the 1.5 H stack, the highest concentrations occurred significantly further downwind of the stack. Concentrations measured near the mean flow reattachment point were highest for the 1.5 H stack. This occurs because emissions near the upper boundary of the cavity region are caught in the general recirculation, which downdrafts the plume towards the reattachment point. Emissions from a lower stack are more rapidly downwashed and dispersed. Thus, this is one case in which a taller stack does not result in lower concentrations. Application of the "2 1/2 times rule" with respect to the terrain feature would, however, result in significantly reduced concentrations downwind because this stack would be well above the cavity region.

Near the downwind end of the cavity (that is, near the reattachment point), the flow is difficult to characterize. Part of the main flow recirculates within the cavity; the rest continues downwind forming a newly de-

veloping boundary layer. The turbulence intensity downwind of the reattachment point is still significantly greater than that found in the undisturbed flow and it decreases with downwind distance. This region can best be characterized by the increased vertical and lateral spreading of a plume over that occurring for a flow without the mountain ridge disruption. The above assertions are generalizations drawn from a limited amount of smoke visualization and mean velocity and turbulence intensity data taken downwind of the reattachment point. Further studies of the behavior of plumes from stacks placed downwind of the reattachment point are needed to further characterize dispersion there.

REFERENCES

American Society of Mechanical Engineers, 1973: Recommended Guide for the Prediction of the Dispersion of Airborne Effluents. Smith, M. (ed.). New York, ASME. 85 p.

Bradshaw, P. and F. Y. F. Wong, 1972: The Reattachment and Relaxation of Turbulent Shear Layer. J. Fluid Mech., 52, 113-135. Part 1.

Briggs, G. A., 1969: Plume Rise. U.S. Atomic Energy Commission, Washington, D.C. Critical Review Series No. TID-25075. 81 p.

Buettner, K. J. K., 1964: Orographic Deformation of Wind Flow. University of Washington, Seattle, Washington. Prepared for U.S. Army Electronics Research and Development Laboratory, Fort Monmouth, New Jersey, under Project No. 1AU-11001-B-021-01, Contract No. DA 36-039-SC-89118. 70 p.

Corby, G. A., 1954: Airflow over Mountains: A Review of Current Literature. Quart. J. Roy. Met. Soc., 80, 491.

Counihan, J., 1969: An Improved Method of Simulating an Atmospheric Boundary Layer in a Wind Tunnel. Atm. Environ., 3, 197-214.

Counihan, J., J. C. R. Hunt, and P. S. Jackson, 1974: Wakes Behind Two-Dimensional Surface Obstacles in Turbulent Boundary Layer. J. Fluid Mech., 64, 529-563. Part 3.

Davenport, A. G., 1963: The Relationship of Wind Structure to Wind Loading. In: Proceedings of Conference on Wind Effects on Buildings and Structures. (National Physical Laboratory, Teddington, Middlesex, England, June, 1963) HMSO, London, 1965. p. 54-102.

Davidson, B., 1963: Some Turbulence and Wind Variability Observations in the Lee of Mountain Ridges. J. Appl. Meteorology, 2(4), 463-472.

Evans, B. H., 1957: Natural Air Flow Around Buildings. Texas Engineering Experiment Station, College Station, Texas. Research Report No. 59.

Gloyne, R. W., 1965: Some Characteristics of The Natural Wind and Their Modification by Natural and Artificial Obstructions. Scientific Horticulture, XVII, 7-19.

Halitsky, J., 1968: Gas Diffusion Near Buildings. In: Meteorology and Atomic Energy- 1968. Slade, D.H. (ed.). U.S. Atomic Energy Commission. Report No. TID-24190. p. 221-255.

Halitsky, J., G. A. Magony, and P. Halpern, 1966: Turbulence Due to Topographical Effects. New York University, New York, Geophysical Laboratory Report No. TR-66-5. 75 p.

Lin, J. T., H. T. Liu, Y. H. Pao, D. K. Lilly, M. Israeli, and S. A. Orsag, 1974: Laboratory and Numerical Simulation of Plume Dispersion in Stably Stratified Flow over Complex Terrain. Flow Research, Inc., Kent, Washington. Prepared for U.S. Environmental Protection Agency, Research Triangle Park, N.C. under Contract No. 68-02-0800. Publication No. EPA-650/4-74-044. 70 p.

Mueller, T. J. and J. M. Robertson, 1963: Modern Developments in Theor. Appl. Mech., 1, 326.

Nagabhushanaiah, H. S., 1962: Separation Flow Downstream of a Plate Set Normal to a Plane Boundary. Ph.D. Dissertation. Colorado State University, Fort Collins, Colo.

Orgill, M. M., J. E. Cermak, and L. O. Grant, 1971: Laboratory Simulation and Field Estimates of Atmospheric Transport - Dispersion Over Mountainous Terrain. Colorado State University, Fort Collins, Colo. Technical Report No. CER70-71MMO-JEC-LOG40.

Petryk, S. and E. Brundrett, 1967: Department of Mechanical Engineering, University of Waterloo. Research Report No. 4.

Plate, E. J., 1967: Diffusion from a Ground Level Line Source into the Disturbed Boundary Layer far Downstream from a Fence. Int. J. Heat and Mass Transfer, 10, 181-194.

Plate, E. J. and C. M. Liu, 1964: The Velocity Field Downstream from a Two-dimensional Model Hill. Part 1. Colorado State University, Fort Collins, Colo. Technical Report No. CER65EJP-CWL41.

Plate, E. J. and C. M. Sheih, 1965: Diffusion from a Continuous Point Source into the Boundary Layer downstream from a Model Hill. Colorado State University, Fort Collins, Colo. Technical Report No. CER65EJP-CMS60.

Pooler, F., Jr. and L. E. Niemeyer, 1970: Dispersion From Tall Stacks: An Evaluation. (Presented at 2nd International Clean Air Congress, Washington, D.C. December 6-11, 1970, Paper No. ME-14D.) 31 p.

Scorer, R. S., 1955: Theory of Airflow over Mountains: IV-Separation of Flow from the Mountain Surfaces. Quart. J. Roy. Met. Soc., 81, 340-350.

Scorer, R. S., 1968: Air Pollution. Oxford Pergamon Press. 151 p.

Sherlock, R. H. and E. A. Stalker, 1940: The Control of Gases in the Wake of Smoke Stacks. Mech. Engr., 62, 455-458.

Snyder, W. H., 1972: Similarity Criteria for the Application of Fluid Models to the Study of Air Pollution Meteorology, Boundary-Layer Meteorology, 3(2), 113-134.

Snyder, W. H., R. S. Thompson, and R. E. Lawson, Jr., 1976: The EPA Meteorological Wind Tunnel: Design, Construction and Operating Details. In preparation for publication in the EPA Environmental Monitoring Series.

Strom, G. H., 1968: Atmospheric Dispersion of Stack Effluents. In: Air Pollution. Vol. I. Stern, A. C. (ed.). New York, Academic Press. Chapter 8.

Sutton, O. C., 1960: Discussion before Institute of Fuels, May 23, 1960. J. Institute Fuel (London), 33, 495.

Tani, I., M. Iuchi, and H. Komoda, 1961: Aeronautical Research Institute, Tokyo, Japan. Report No. 364.

Tillman, W., 1945: Volkenrode translation MAP - VG 34 - 45T. British Ministry of Aircraft Production, London, England.

World Meteorological Organization, 1967: The Airflow over Mountains. WMO, Geneva, Switzerland. Report No. 98. 43 p.